Geophysical Journal International

Geophys. J. Int. (2015) **201,** 1743–1764
GJI Geodynamics and tectonics

doi: 10.1093/gji/ggv104

Absolute plate motion of Africa around Hawaii-Emperor bend time

S. M. Maher,[1] P. Wessel,[1] R. D. Müller,[2] S. E. Williams[2] and Y. Harada[3]

[1] *Department of Geology and Geophysics, School of Ocean and Earth Science and Technology, University of Hawaii at Mānoa,* 1680 *East-West Road, Honolulu, HI* 96822, *USA. E-mail: sarahxmaher@gmail.com*
[2] *EarthByte Group, School of Geosciences, Madsen Building F*09, *University of Sydney, NSW* 2006, *Australia*
[3] *School of Marine Science and Technology, Tokai University,* 3-20-1, *Orido Shimizu Shizuoka* 424-8610, *Japan*

Accepted 2015 February 27. Received 2015 February 18; in original form 2014 September 12

SUMMARY

Numerous regional plate reorganizations and the coeval ages of the Hawaiian Emperor bend (HEB) and Louisville bend of 50–47 Ma have been interpreted as a possible global tectonic plate reorganization at ∼chron 21 (47.9 Ma). Yet for a truly global event we would expect a contemporaneous change in Africa absolute plate motion (APM) reflected by physical evidence distributed on the Africa Plate. This evidence has been postulated to take the form of the Réunion-Mascarene bend which exhibits many HEB-like features, such as a large angular change close to ∼chron 21. However, the Réunion hotspot trail has recently been interpreted as a sequence of continental fragments with incidental hotspot volcanism. Here we show that the alternative Réunion-Mascarene Plateau trail can also satisfy the age progressions and geometry of other hotspot trails on the Africa Plate. The implied motion, suggesting a pivoting of Africa from 67 to 50 Ma, could explain the apparent bifurcation of the Tristan hotspot chain, the age reversals seen along the Walvis Ridge, the sharp curve of the Canary trail, and the diffuse nature of the St. Helena chain. To test this hypothesis further we made a new Africa APM model that extends back to ∼80 Ma using a modified version of the Hybrid Polygonal Finite Rotation Method. This method uses seamount chains and their associated hotspots as geometric constraints for the model, and seamount age dates to determine APM through time. While this model successfully explains many of the volcanic features, it implies an unrealistically fast global lithospheric net rotation, as well as improbable APM trajectories for many other plates, including the Americas, Eurasia and Australia. We contrast this speculative model with a more conventional model in which the Mascarene Plateau is excluded in favour of the Chagos-Laccadive Ridge rotated into the Africa reference frame. This second model implies more realistic net lithospheric rotation and far-field APMs, but fails to explain key details of the Atlantic Ocean volcanic chains. Both models predict a Canary plume influence beneath the Madeiras. Neither model, when projected via the global plate circuit into the Pacific, predicts any significant change in plate motion around chron 21. Consequently, Africa APM models do not appear to provide independent support for a chron 21 global reorganization.

Key words: Plate motions; Dynamics of lithosphere and mantle; Dynamics: gravity and tectonics; Africa.

1 INTRODUCTION

There is growing evidence for a tectonic plate reorganization on a global scale around 50 Ma (Morra *et al.* 2013), or more likely closer to chron 21 (47.9 Ma). This time period includes the Australian–Antarctic Plate reorganization (Whittaker *et al.* 2007, 2013) and the dramatic slowdown of the India Plate (Copley *et al.* 2010; Cande & Patriat 2015). In the Pacific region this tectonic activity is concurrent with the South Pacific triple-junction reorganization (Cande *et al.* 1982). The Hawaiian Emperor bend (HEB), which has been dated around chron 21 (O'Connor *et al.* 2013) (but could possibly have started a few Myr earlier, e.g. Sharp & Clague 2006) exhibits a 120° bend in the volcanic chain which has traditionally been interpreted to indicate a significant, 60° change in Pacific Plate motion as it passed over the Hawaiian hotspot (Duncan & Clague 1985; Koppers *et al.* 2001; Wessel & Kroenke 2008). However, this interpretation is now considered controversial. Palaeomagnetic evidence from the Emperor seamounts suggest the plume could have drifted 10–15° south (Tarduno *et al.* 2003), and if so the HEB predominantly would be a product of hotspot motion and not a change in the Pacific absolute plate motion (APM; Tarduno *et al.* 2009). Still, coeval samples from the Hawaii chain and Louisville chain in the

south Pacific show no significant change in hotspot separation for the past 55 Ma (Wessel & Kroenke 2009), and recent age dates from the Louisville bend constrain its timing to be coeval with the HEB (Koppers *et al.* 2012). While plume motion appears to be a major cause of the HEB geometry, it seems less significant for Louisville (Koppers *et al.* 2012). Thus, it is probable that at least a component is related to plate motion changes (O'Connor *et al.* 2013), but this may be a minor, rather than a major component of the HEB.

In contrast, the APM of Africa represented by previous models does not exhibit a major change in motion around chron 21. The plate has less distinct hotspot trails, slower movement, and fewer quality age determinations when compared with the Pacific domain, making its motion much harder to define. Yet, there are numerous indicators that a change in Africa Plate motion did occur sometime during chron 20–23, such as the change in plate motions of both North and South America relative to Africa (Müller *et al.* 1999) and the sigmoidal fracture zone bends observed between Africa and Antarctica (Cande *et al.* 2010). Similar fracture zone bends are also seen in the Weddell Sea, where they describe distinct relative plate motion (RPM) changes between South America and Antarctica at chrons 30 and 21 (Livermore *et al.* 2005). Whether these changes observed at different spreading centres are truly synchronous at chron 21 is not yet proven but the case for it is strengthening (Cande & Patriat 2015). However, for our purposes they are essentially synchronous given the much larger uncertainties in the timing of APM models, which depends on age dating of volcanic samples. Cande & Stegman (2011) recently suggested the APM of Africa might briefly have been retarded as a consequence of Réunion plume push. This would cause Africa to 'pivot', meaning that its stage poles are within the plate polygon. It is thus possible that the APM of Africa remains incompletely understood.

Africa plays a key role in global plate reconstructions because of its stability over time, surrounded by long-lived, divergent plate boundaries (e.g. Seton *et al.* 2012). These boundaries produce seafloor whose fabric and magnetic anomalies reflect clear relative plate motions with respect to neighbouring plates. The continent traverses very slowly over the mantle, and over the past 100 Ma it has only moved 500–900 km (Torsvik *et al.* 2008). The eastern margin of Africa began rifting from the Gondwana supercontinent in the early Jurassic period, after volcanism along the Karoo Rift ceased (e.g. Cox 1992). In the early mid-Jurassic spreading between Antarctica and Madagascar created the East Africa margin. Rifting between Africa and South America originated at the southernmost part of the continents at ~190 Ma and propagated northward (e.g. Daly *et al.* 1989; Nürnberg & Müller 1991). Seafloor spreading was initiated along the Mid-Atlantic Ridge, forming the Atlantic Ocean (Cande *et al.* 1988; Nürnberg & Müller 1991). More recent episodes of spreading include the rifting between the Seychelles microcontinent and Madagascar by the start of chron 27n (Collier *et al.* 2008), and the formation of the Mascarene Basin via seafloor spreading (e.g. Schlich 1982). There is some debate over when the fossil ridge in the Mascarene Basin went extinct, identifying the youngest seafloor age at chron 27n (Collier *et al.* 2008), or 68 Ma in the northern portion of the basin and 59 Ma in the south due to a southward propagating ridge extinction (Bernard & Munschy 2000). However, more recent investigations suggest the extinction of the ridge occurred around 61 Ma (Eagles & Wibisono 2013). Ongoing relative motion between the Nubia and Somalia plates over the past 11 Ma has resulted in ~100 km of motion (Royer *et al.* 2006). In general, RPMs between Africa and its neighbours are well understood and all of the major tectonic plates, except for those in the Pacific Basin, can be linked via rifting or seafloor spreading going back to 200 Ma (Seton *et al.* 2012).

Because of its perceived stability, many plate reconstruction models use Africa as an anchor plate. From this reference frame, the absolute motions of the other plates are derived through RPM models, so it is desirable to know its APM with high accuracy. The APM of a plate reveals how it moved over time relative to a fixed point in the mantle reference frame, usually defined by a set of hotspots. APM models use hotspots as either fixed or moving points to determine how the plate has moved relative to the mantle, utilizing volcanic chains on the plate as physical evidence for its past motion. In a fixed hotspot framework, the plate travels over a set of stationary hotspots so the impinging mantle plumes cause relatively focused surface volcanism, creating volcanic chains that display colinear age progressions. By fitting the geometry and age progressions of at least two hotspot chains on the plate, its motion over time can be determined. Recent models can also accommodate an amount of hotspot motion as predicted by mantle flow models while simultaneously fitting the geometry, age progression, and palaeolatitudes of volcanic chains (e.g. O'Neill *et al.* 2005; Doubrovine *et al.* 2012).

Several differing models of Africa APM have been proposed, but no single model can fully explain the volcanic features observed on the plate itself, and none predict a major change in plate motion at chron 21. Apart from the strong evidence from RPM studies, the geometry of key hotspot chains may provide significant evidence for changes in APM, including the inverted 'C'-shaped curve of the Canary chain with a recent bend that appears to have been initiated around 20 Ma. More importantly, if a ridge-centred Réunion hotspot created both the Mascarene Plateau and Chagos-Laccadive Ridge simultaneously, it could have potentially formed the ~115° observed bend in the Réunion-Mascarene chain (Harada & Wessel 2003), which may be the equivalent of the HEB on the Africa Plate (Fig. 1). If confirmed, this bend would reflect a clear-cut chron 21 change in the APM of Africa, adding credence to the idea of a global plate reorganization at that time. A complementary ~145° bend is also observed on the Chagos-Laccadive Ridge (Fig. 1) near ODP Site 713 (46.2–48.8 Ma, Vandamme & Courtillot 1990), evidence for a chron 21 event affecting India Plate motion and reflected in India–Africa RPM (Cande & Patriat 2015).

We believe it is important to distinguish between Africa APM models in general (e.g. Torsvik *et al.* 2008; Doubrovine *et al.* 2012) that use Africa as the anchor plate in a global study and studies that focus specifically on the Africa APM, such as ours, as this allows different questions to be asked. While many studies have published models for African APM (and we will review the most important ones below), not many focus on the APM of the Africa Plate in isolation from trails on other plates. For example, the recent global APM model of Doubrovine *et al.* (2012) uses hotspots from the Pacific, hence its predictions cannot be used for an independent test of changes in Africa APM at HEB time. Consequently, we believe an assessment of African APM based almost entirely on data from the Africa Plate alone is of considerable value.

In this paper, we explore key observational features on the Africa Plate that need to be explained by APM models. Following a review of past models and a preliminary exploration of required stages of motion and the tectonic implications of these stages, we present available data and proceed to model the trails produced by four key hotspots on the Africa Plate using a modified version of the hybrid polygonal finite rotation method (PFRM; Wessel & Kroenke 2008). Because of the controversial nature of Réunion trail interpretations, two separate APM models have been created to fit these features: a speculative model (A) will test if a major chron 21 APM change

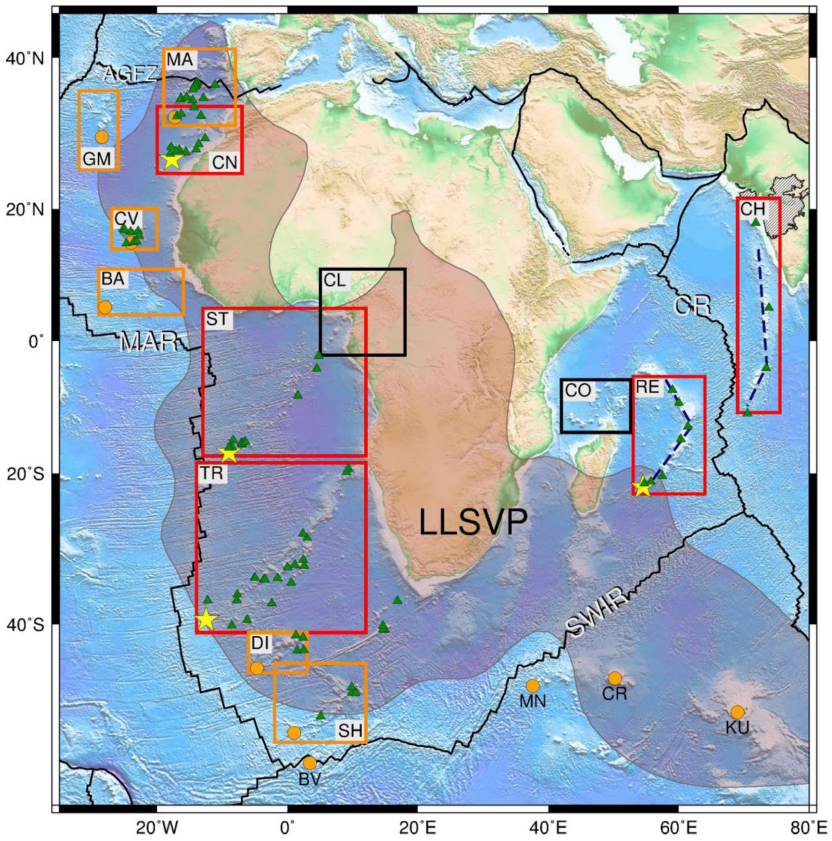

Figure 1. Hotspot chains on the Africa Plate. Yellow stars represent hotspots used to constrain our models; other hotspots are shown as orange circles. Abbreviations for chains are listed in Table 1. Green triangles are locations of dated seamounts. Labelled rectangles indicate the seafloor areas affected by the respective hotspots. Africa divergent plate boundaries are the Mid-Atlantic Ridge (MAR) between Africa and the Americas, Carlsberg Ridge (CR) denoting the India Plate boundary, the Southwest Indian Ridge (SWIR) defining the Antarctic Plate boundary, and the Azores-Gibraltar Fracture Zone (AGFZ) between Africa and Eurasia. The Shaka Ridge (SR), Bouvet (BV), Marion (MN), Crozet (CR) and Kerguelen (KU) hotspots are also labelled. Hachured area denotes the Deccan Traps, and red-grey area describes the large low shear wave velocity province (LLSVP, Torsvik *et al.* 2014). Dashed lines identify the chron 21 bends in the Chagos-Laccadive and Réunion chains; see text for discussion.

Table 1. Abbreviations for hotspot chains.

Name	Abbreviation
Bathymetrist	BA
Chagos-Laccadive	CH
Canary	CN
Cape Verde	CV
Discovery	DI
Great Meteor	GM
Madeira	MA
Shona	SH
St. Helena	ST
Tristan	TR
Réunion	RE

(presumed to be reflected in the Réunion-Mascarene bend) could be a tectonic possibility, while a more conventional model (B) will omit that feature in favour of including the Chagos-Laccadive Ridge. We examine the viability of these models by comparing them to published models, examining their impact on global APM velocities, determining the net lithospheric rotation they imply, and projecting them into the Pacific Plate reference frame for comparing their predictions for the Hawaii-Emperor trail.

2 HOTSPOT CHAINS ON THE AFRICA PLATE

Burke & Wilson (1976) identified 43 hotspots on the Africa Plate, 8 of which are in oceanic intraplate settings and an additional 10 are located close to ocean ridges (Fig. 1). More recently Courtillot *et al.* (2003), using several criteria to diagnose a potentially deep mantle origin, settled on just three Africa Plate hotspots. In their view, the major candidates were Afar, Réunion and Tristan with lower status assigned to the Canary and Cape Verde chains. While the continental Afar hotspot has not produced a suitable trail for modelling, we will discuss the others and several additional volcanic provinces on the Africa Plate. We will demonstrate that these hotspots show evidence of being plume-related and could offer critical constraints on a new Africa APM.

2.1 Tristan–Walvis

Tristan-Walvis (TR; Fig. 1) is the longest-lived hotspot chain on the Africa Plate, originating between 129 and 133 Ma (e.g. O'Connor & Duncan 1990; O'Neill *et al.* 2005); its hotspot is believed to be presently located near the Tristan da Cunha Island. Proximity to the Mid-Atlantic Ridge during the Cretaceous resulted in two hotspot trails: the Rio Grande Rise on the South America Plate

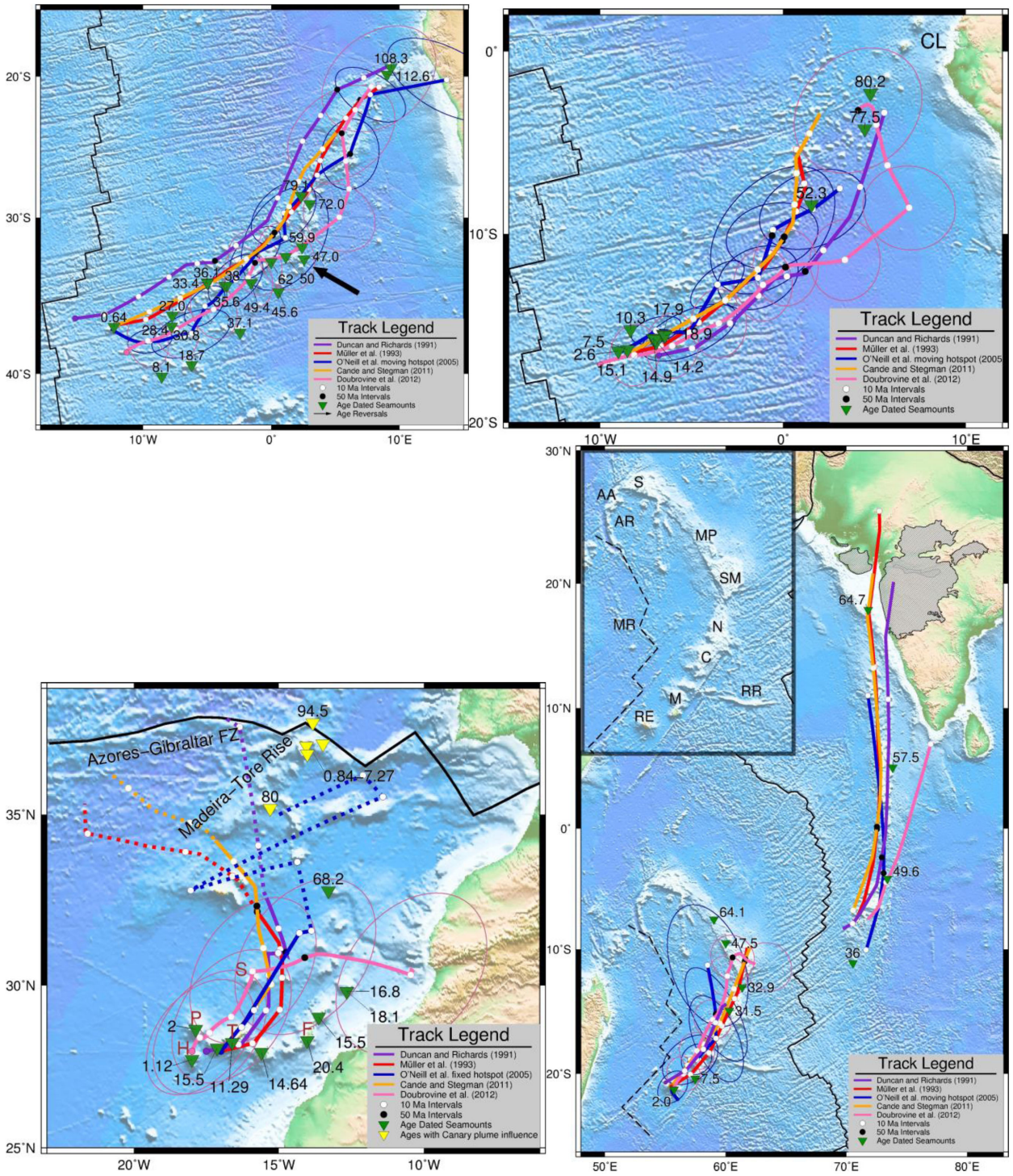

Figure 2. Previous model predictions for Africa hotspot trails, with select observed ages as green triangles. See legends for symbol details. (a) The Tristan hotspot trail. Hotspot location for the O'Neill *et al.* (2005) model was stated to be Tristan da Cunha Island. Hotspot location for Duncan & Richards (1991) model was determined from Fig. 3 in their paper. (b) St. Helena hotspot trail. Hotspot location for Duncan & Richards (1991) model was determined from Fig. 3 in their paper. Müller *et al.* (1993) hotspot location was chosen for best local fit, and the same hotspot location was used for Cande & Stegman (2011). The Cameroon Line (CL) overrides the oldest portion of the St. Helena chain in the north. (c) The Canary hotspot trail. Dashed lines indicate the trail extended to 80 Ma when data was available. Madeira age samples displaying Canary plume influence (Geldmacher *et al.* 2006) are shown as yellow triangles. Hotspot location for Duncan & Richards (1991) model was determined from Fig. 4 in their paper. Müller *et al.* (1993) hotspot location was chosen for best local fit, and the same hotspot location was used for Cande & Stegman (2011). O'Neill *et al.* (2005) did not include an estimate on Canary hotspot motion, so their fixed hotspot APM was used and hotspot location was chosen for best local fit. Locations for Tenerife (T), La Palma (P), el Hierro (H), Fuerteventura (F) and Selvagem (S) Islands are shown. (d) Réunion and Chagos-Laccadive hotspot trails. Duncan & Richards (1991) hotspot location estimated from Fig. 5 in their paper. The Deccan Traps (hachured) denotes the onset of the Réunion hotspot plume. The insert shows the location of key features on or near the Réunion hotspot track: the Seychelles microcontinent (S), Amirante Ridge (AR), Amirante Atolls (AA), Mascarene Plateau (MP), Saya de Malha Bank (SM), Mascarene Ridge (MR), Nazareth Bank (N), Caragados Carajos Bank (C), Mauritius Island (M), Réunion Island (R) and the Rodriguez Ridge (RR).

and the Tristan chain on the Africa Plate. Two apparently distinct trails, the Gough Lineament and the Walvis Ridge, were formed as parts of the Tristan-Walvis chain. There are several hypotheses for how these trails have formed, including the presence of two hotspots (O'Connor & Duncan 1990) or spatial zonation of the hotspot plume (Deppe *et al.* 2010). The hotspot pair explanation seems unlikely because of the close proximity of these segments, and the spatial zonation explanation is a case of special pleading for the Tristan chain, which lessens the arguments for a plume origin (Anderson 2001). Consequently, current models of Africa APM have not addressed this bifurcation, typically choosing instead to follow the northern lineament along the Walvis Ridge (Fig. 2a). Age dating along the Walvis Ridge has revealed age reversals of more than 10 Ma between seamounts in relatively close proximity where a linearly increasing age progression would be expected. Newly redated samples (Rohde *et al.* 2013) confirm the existence of anomalously young volcanism on the Walvis Ridge and Rio Grande Rise. These anomalies might be explained by uncertainties in the ages themselves, sampling biases in between dredge sites, simultaneous volcanism in different areas along the chain, or a large diameter plume conduit (O'Neill *et al.* 2005). Alternatively, it could be an indication of an aspect of Africa APM not presently understood or modelled.

2.2 St. Helena

Approximately 2000 km north of the Tristan chain we find the St. Helena hotspot chain (ST; Fig. 1), which displays a linear age progression from the present day to ~80 Ma. Any older seamounts would have been overprinted by more recent Cameroon Line volcanism. Courtillot *et al.* (2003) described St. Helena as a non-primary hotspot with no lower mantle origin, unrelated to plume volcanism. The chain is manifested as a diffuse trail up to 500 km wide in some locations and is characterized by low-amplitude seafloor volcanic features. This confused expression could be due to the presence of through-cutting fracture zones acting as zones of weakness and allowing for a broader zone of hotspot volcanism (O'Connor & Le Roex 1992). Most of the dated seamounts are concentrated at the young end of the chain, presenting uncertainties in the details of age progression for the older section (Fig. 2b). Despite Courtillot *et al.*'s (2003) assessment, we choose to include it in the modelling in order to provide broad spatial coverage of hotspots on the plate. As further justification, we note this hotspot lies near the perimeter of the large low shear velocity province from which the majority of the Indo-Atlantic plumes appear to originate (Burke *et al.* 2008).

2.3 Canary

The Canary chain (CN; Fig. 1), located northwest of the African continent, has a distinctive inverted 'C' shape, presumably due to its close position to the Euler poles describing Africa APM. It appears to have originated at ~67 Ma, though the influence of the plume has been detected geochemically within the Madeira-Tore Rise going back to the Cretaceous (Geldmacher *et al.* 2006). Models of Africa APM (Fig. 2c) often fail to accurately recreate this shape, leading to alternative non-hotspot explanations for this mismatch, such as intraplate deformation (Steinberger *et al.* 2004) or edge-driven convection cells interacting with the Canary plume (Geldmacher *et al.* 2005). There is also an abundance of recent volcanism, with Tenerife, La Palma and el Hierro islands all experiencing volcanic activity within the past 100 yr. While this may be expected given a slow APM and hence close proximity of the hotspot to its volcanic offspring, it makes the onset of hotspot volcanism at points along the chain more difficult to determine.

2.4 Réunion

The Réunion hotspot trail (RE; Fig. 1) started with the arrival of the plume head in the Deccan Traps at ~67 Ma, forming the Chagos-Laccadive Ridge on the India Plate before it was overrun by the Carlsberg Ridge and producing volcanism on the Africa Plate as well (Duncan & Richards 1991). Previous models generally predict the hotspot first to have formed the Saya de Malha Bank, then the Nazareth and Caragados Carajos Banks further south and finally the Mauritius and Réunion Islands (Fig. 2d). There is some controversy over a submarine plateau, referred to in this paper as the Mascarene Plateau, which extends to the northwest from the Saya de Malha Bank to connect with the Seychelles microcontinent (Fig. 2d). Three seismic profiles along the ridge have indicated flat lying sedimentary beds which could be interpreted as the upper levels of the plateau consisting of carbonate banks (Bunce & Chase 1966), and it has been recently proposed that the plateau, Chagos-Laccadive Ridge, the Saya de Malha Bank, Nazareth Bank and Mauritius are actually continental fragments (Torsvik *et al.* 2013). Alternatively, a drill site along the Mascarene Plateau found massive basalt basement rocks from the early Palaeocene (Backman *et al.* 1988) associated with a weak magnetic anomaly, causing the hypothesis to be posed that it was a more deeply buried portion of the volcanic ridge to the south (Bunce & Chase 1966). Seismic refraction on Saya de Malha indicated a crustal composition intermediate between continent and ocean, with the base displaying a seismic velocity close to that of Pacific volcanic islands (Fisher *et al.* 1967). Volcanic activity on the Seychelles ranged from ~61 to 67 Ma, had a hotspot origin, and the reconstructed volcanic region lay nearly radially above the plume generation zone during the eruption of the Deccan Traps (Ganerød *et al.* 2011), so it is not unreasonable to suspect that the Mascarene Plateau could partly have been formed by hotspot volcanism. Additionally, it is unknown how long the Réunion hotspot was centred below or near the Carlsberg Ridge, during which time the Mascarene Plateau could have developed contemporaneously with the Chagos-Laccadive Ridge. Gravitational admittance analysis supports this possibility as elastic thickness estimates imply the first 30 Myr of hotspot volcanism formed on juvenile lithosphere (Tiwari *et al.* 2007). There is limited age data along the Réunion hotspot track, which has made pinpointing the exact hotspot position at chron 21 difficult. The region is also complicated by seafloor spreading in the Mascarene Basin, which terminated with the extinction of the Mascarene Ridge (Fig. 2d) within a few Myr of the onset of the Réunion hotspot (Bernard & Munschy 2000; Eagles & Wibisono 2013). While the timing is similar, it appears that the seafloor on which the Réunion hotspot produced its volcanic edifices was fixed to the rest of the Somalia Plate when the volcanism occurred, making a simple one-plate Africa model possible. Additionally, more recent but limited motion between Nubia and Somalia would have introduced some motion bias on the order of 100 km (Royer *et al.* 2006).

2.5 Other hotspot chains not used for modelling

Several other hotspot chains are present on the Africa Plate but were not used to constrain the fit for the new hotspot model for various reasons (i.e. lacking ages, being relatively short-lived, etc.). We will

instead use these trails for model validation purposes. These chains are detailed below.

The Cape Verde hotspot chain (CV; Fig. 1) is a more recent hotspot but its oldest volcanism is not well constrained. The earliest date was reported as 26 Ma on Sal using K–Ar dating techniques, though current Ar/Ar dating has given Sal an age of ∼17 Ma, and the most recent volcanism in the chain was 0.3 Ma (Holm *et al.* 2008). Episodic volcanism is common among all the islands within this chain and can last for several million years. Its close proximity to the Africa Plate Euler poles means very little motion is expected, and this may be reflected in the observed overprinting, making the onset of volcanism difficult to determine. The presence of a significant swell suggests it is caused by a mantle plume (McNutt 1988).

The Bathymetrists seamount chain (BA; Fig. 1) in the Equatorial Atlantic has a general southwest to northeast trend off the Sierra Leone coast of Africa. Zircon dates of ∼58 Ma from the Carter seamount at the older end of the chain reveal that the volcanic chain probably formed in the early Eocene (Skolotnev *et al.* 2010). While it does have a distinct track compatible with APM predictions, no Ar/Ar ages have been obtained along the chain so the lifespan of the hotspot cannot be established.

The New England hotspot has been quite prolific in the formation of seamounts, first creating the White Mountains and Corner Seamount chains on the North American Plate (Duncan 1984), then the Great Meteor chain on the Africa Plate (GM; Fig. 1). The most recent volcanism has been on the Great Meteor seamount with an age of 17.32 Ma (Geldmacher *et al.* 2006). No other ages have been measured in the Great Meteor chain to the north, though recurrent volcanism has been observed. Several of the seamounts could have formed simultaneously (Tucholke & Smoot 1990), so the geometry of the chain would not be a reliable constraint on the fit of our model.

The Madeira hotspot chain (MA; Fig. 1) is just to the north of the Canary hotspot chain and crosses the Azores-Gibraltar Fracture Zone onto the Eurasia Plate. It has been extensively sampled for age dates. Younger (mid-Miocene–Pleistocene) volcanism is superimposed on a much older (late Cretaceous) basement most likely related to the Canary hotspot (Geldmacher *et al.* 2006). However, the proximity of the Africa-Eurasia Plate boundary contributes to weak lithospheric zones and tectonic deformation that could affect the location and orientation of volcanism (Geldmacher *et al.* 2005), obscuring the true hotspot trail. The Canary chain shows a much clearer age progression and orientation, and its close proximity to the Madeira chain means the latter would exhibit a similar hotspot track and add minimal new information to constrain the final model.

The Shona (SH), Discovery (DI) and Bouvet (BV) hotspots are all located to the south of the Tristan chain near the Mid Atlantic Ridge (Fig. 1). Recent age samples from Shona and Discovery chains indicate the trails initiated only ∼44–41 Ma and have a northeast age-progressive trend (O'Connor *et al.* 2012). While these hotspot trails show the general trend of the Africa Plate after 40 Ma, they do not add new constraints on the parameters of our plate motion model. The nearby Bouvet hotspot trail has been difficult to resolve due to the influence of the Southwest Indian Ridge and Shaka Ridge. Without age dates along the ridge and a distinct trail the geometry cannot be separated from nearby formations (O'Connor *et al.* 2012).

The Marion (MN) hotspot trail originated on southeast Madagascar at ∼90 Ma (Torsvik *et al.* 1998), with a vague trace winding southward along the Madagascar plateau to a ridge-shaped bathymetry anomaly slightly north of the Southwest Indian Ridge (SWIR). Then, the trace crosses the SWIR to the Antarctica Plate before reaching Marion Island (Duncan & Richards 1991). However, its current location on another plate means that RPMs would have to be taken into account to fit the unclear and undated hotspot trail on Africa, making it an unreasonable choice to fit in our modelling.

The Crozet (CR; Fig. 1) hotspot is presently located under the Antarctic Plate, 750 km away from the Southwest Indian Ridge. Its trail consists of five islands and islets composing the Crozet Archipelago and an underlying basaltic plateau dated at 54 Ma. The Crozet bank supporting the archipelago is considered the current position of the hotspot plume, with volcanism going back to the SWIR in the early Eocene (Breton *et al.* 2013). Crozet's position on the Antarctic Plate and the lack of Ar/Ar age dates make it too problematic to incorporate in the fit of the models.

The Comores hotspot chain (CO; Fig. 1) lies to the north of Madagascar and is composed of the Comores Islands and potentially extending back through the Farquhar and Armirante atolls before terminating at the Seychelles microcontinent. K/Ar age dates of the Comores Islands reveal an increasing age moving eastward, but the more recent northwest trend of the hotspot trail is inconsistent with all current models. Instead this orientation is attributed to the relative plate motions between Nubia and Somalia over the past 10 Ma (Emerick & Duncan 1982). Its deviating trend means it is unlikely to reflect motion of another hotspot in such close proximity to Réunion, hence another tectonic explanation is more likely; we therefore chose not to include this chain in our modelling.

Finally, the Cameroon Line (CL; Fig. 1) is a volcanic trail that originates in continental Africa, with its youngest features potentially overwriting the oldest portion of the St. Helena hotspot trail. Recent studies indicate that the source of volcanism is due to lithospheric instabilities caused by top-down cooling (Milelli *et al.* 2012). The lack of age progression along the trail and recurrent volcanism along its entire continental length within a zone of earlier lithospheric thinning (e.g. Reusch *et al.* 2011; Heine & Brune 2014) agues against a mantle plume origin, hence the trail was not used for modelling.

3 PREVIOUS MODELS

The first APM model for Africa was created by Morgan (1981) in which the plate was positioned over a hotspot reference frame defined by the Canary, Tristan, Crozet, Réunion, and Kerguelen hotspots. All hotspots appeared to be stationary within 5°, and much of the scatter was assumed to be due to errors in the plate motion reconstructions incorporated into the model. Morgan predicted that better models of seafloor spreading would see some of that scatter eventually disappear (Morgan 1981). O'Connor & Duncan (1990) expanded the Africa APM model by using ages along Walvis Ridge of the Tristan hotspot chain. They extrapolated the hotspot trails by assuming that hotspots are fixed relative to one another and the basement ages and geometry of the Walvis Ridge accurately represent the APM. It also predicted that the Réunion hotspot followed the trend from Réunion Island to the Saya de Malha Bank between 0 and 36 Ma, but moved more slowly than expected based on the age dates. This discrepancy could be due to motion between the Réunion and Tristan hotspots or RPM occurring in the African Rift Zone (O'Connor & Duncan 1990).

More recent model predictions are presented in Fig. 2. Radiometric ages and the geometries of the Walvis Ridge and the Cameroon Line were key observations constraining the Duncan & Richards (1991) APM model. Their model then predicted the age

progression and geometry of the Mascarene Ridge in the Réunion trail and the Madagascar Ridge of the Crozet hotspot trail. The agreement between the predicted and observed hotspot trails gave credence to the idea that hotspots move very slowly in the Indo-Atlantic reference frame, concluding that hotspots have remained fixed for the past 60 Ma. There was also excellent agreement along the Réunion hotspot trail (Fig. 2d) if the hotspot was centred at a seamount to the west of Réunion Island (Duncan & Richards 1991).

O'Connor & Le Roex (1992) incorporated the Gough lineament and Walvis Ridge from the Tristan hotspot trail along with the St. Helena and Réunion hotspots to revise the Africa APM model. The predicted Tristan hotspot trail followed a more northerly route than its predecessors, and the APM exhibited a slower plate velocity from 40 Ma to present day and between 120 and 80 Ma than previous models, though it does not fit the St. Helena hotspot chain particularly well. The predicted age distribution along the Réunion chain was significantly different from the recorded ages, which could be due to the location of the hotspot used (O'Connor & Le Roex 1992), or that a fossil spreading axis under Réunion created a different route for plume melt (Bonneville *et al.* 1988).

Müller *et al.* (1993) constrained a new APM model by incorporating 11 hotspot trails from Africa and several of its neighbouring plates. Hotspot track segments were considered simultaneously by using the relative plate motions for a particular age range. In this way, ages and geometry for the Chagos-Laccadive Ridge were incorporated into the Réunion hotspot track. The study concluded that there was no major motion between the Indo-Atlantic hotspots going back 84 Ma (Müller *et al.* 1993).

The hypothesis of moving hotspots was proposed to explain several inconsistencies that had resulted when using a fixed hotspot reference frame, including the inability to explain anomalous palaeolatitudes in the Emperor seamount chain (Tarduno *et al.* 2003) and the difficulty to reconciling the Atlantic and Pacific hotspot reference frames (Molnar & Stock 1987). O'Neill *et al.* (2005) were the first to incorporate moving hotspots into an Africa APM model, modelling plume and plate motions back to 120 Ma. Dynamic simulations of plume motion were created and constrained using plate kinematics, tomography and sparse palaeomagnetic data. Whenever there was an observed age reversal along the Tristan chain the oldest reliable age was used. The preferred moving hotspot model yielded reasonable motions and broadly satisfied the available palaeolatitude and geochronology data. However, predictions from moving and fixed hotspot reference frames were not significantly different above their uncertainties since 80 Ma, but required larger hotspot motions (5°–10°) for times prior to 80 Ma (O'Neill *et al.* 2005).

Cande & Stegman (2011) recently created an Africa APM by summing the APM of Antarctica (Müller *et al.* 1993) and a new RPM model describing motion between Africa and Antarctica (Cande *et al.* 2010). Their APM predicted a better fit to the Great Meteor and Tristan hotspot chains than that of the Müller *et al.* (1993) model when using the same hotspot locations, but showed little difference in the Réunion hotspot track (Cande & Stegman 2011). Neither model fits the Canary chain particularly well.

A new moving hotspot global APM model was created by Doubrovine *et al.* (2012) using five hotspots chosen for their clear age progressions and well-defined tracks in the Atlantic (Tristan-Walvis and New England), Pacific (Hawaii and Louisville) and Indian (Réunion) oceans. Plume motion was determined by numerical modelling of whole mantle convection combined with the advection of plumes into the mantle flow field. The resulting framework of moving hotspot locations was then used to create a global APM model going back to 80 Ma (Doubrovine *et al.* 2012). The predicted hotspot track for Réunion was examined in detail by Torsvik *et al.* (2013), who analyzed zircons found on the island of Mauritius and proposed that several key features of the Réunion hotspot track were also continental fragments from Madagascar and India. For the past 50 Ma the Réunion hotspot trail has then coincidentally followed the alignment of these fragments. If these features are indeed continental, then any APM model based on this hotspot trail would necessarily be suspect (Torsvik *et al.* 2013).

Several complications with the current models need to be addressed. Rifting between the Nubia and Somalia plates (Royer *et al.* 2006) may have moved positions up to ∼100 km, and the late development of the Mascarene Basin (Bernard & Munschy 2000; Eagles & Wibisono 2013) may have caused minor relative plate motion between the Réunion trail on the Somalia Plate and the rest of the Africa hotspot trails (on the Nubia Plate). Plume-ridge interactions (Small 1995) could have affected the geometry of several hotspot chains, including Tristan, Réunion, and the Madeiras, thus biasing any modelling attempts. Lithospheric striations could potentially increase seamount chain dispersion, particularly along the St. Helena track (O'Connor & Le Roex 1992). The distribution of seamount ages can also be obscured by dredging techniques, which typically collect the younger material on the outer surface of the seamount, making the actual date of onset volcanism difficult to determine for such a slow moving plate (O'Connor & Le Roex 1992). In terms of constraining hotspot motion, the only available palaeolatitude data are from the Tristan and Réunion chains. The latter has a predicted northern motion of 8 mm yr^{-1} (Vandamme & Courtillot 1990), while Tristan has a 4–7° anomaly (Sager & Tominaga 2008) or 10° of southward motion from 130 to 80 Ma followed by relatively no movement (Hall & Bird 2007). In general, the slow-moving nature of the plate and limited and unreliable sampling of seamounts has made the motion of the Africa Plate much less constrained when compared with APM models for the Pacific Plate.

4 KEY PLATE TECTONIC EVENTS AFFECTING THE AFRICA PLATE

All published APM models show a general trend of Africa moving northeast over time. Yet, several features formed on the Africa Plate during four time intervals may reflect more or less abrupt plate motion changes: (1) based on inferred volcanic propagation rates along the St. Helena chain O'Connor *et al.* (1999) suggested that plate velocity had slowed 33 per cent by 19 Ma. This change may correlate with the observed bend in the Canary chain near Fuerteventura, dated around 20 Ma (O'Connor *et al.* 1999). The trend for the last 20 Ma in the northern part of the plate is more east–west than earlier alignments; (2) before the apparent 20 Ma bend (back to ∼50 Ma), the APM should align with the more north-south orientation of the Canary trail geometry without distorting predictions elsewhere; (3) fracture zone bends between Africa and Antarctica reflect a substantial change in relative plate motion at chron 30 (Cande *et al.* 2010) which coincides with the onset of Réunion hotspot volcanism in the Deccan Traps (Chenet *et al.* 2007) and the termination of the Réunion-Mascarene trail at the Seychelles microcontinent, respectively. This time interval corresponds to the formation of the Mascarene Plateau and the Chagos-Laccadive Ridge. While the relative plate motions clearly changed at both ends of this time interval, assuming the Réunion trail continues up the Mascarene Plateau toward the Seychelles is nevertheless speculative. We will therefore test two hypotheses of APM during this interval: one (model A)

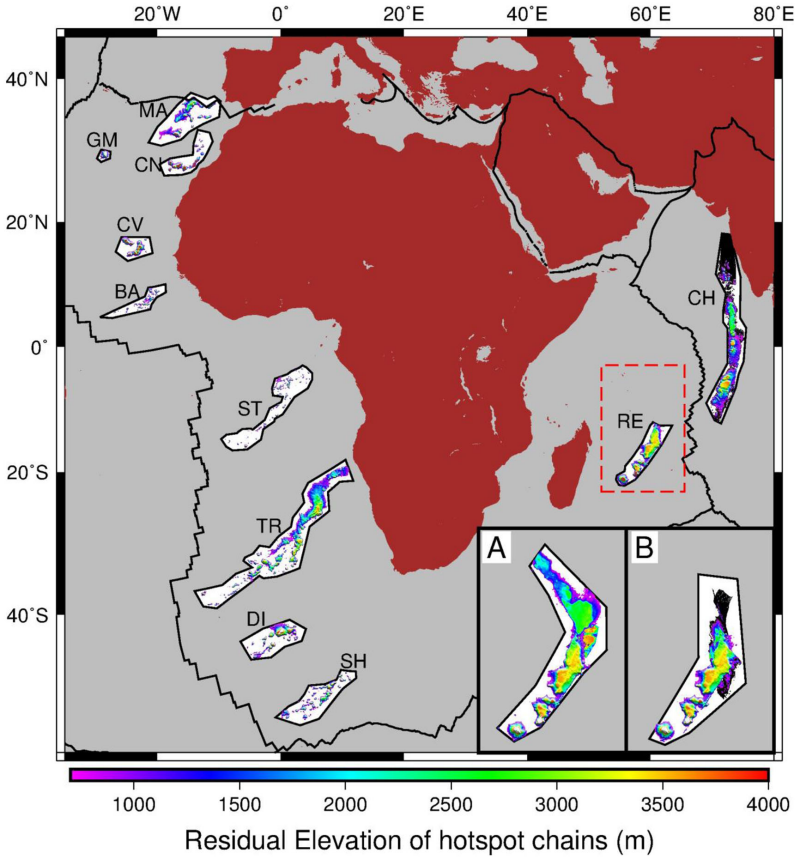

Figure 3. Residual topography of seamount chains. Envelopes for each chain are shown in light grey, along with the elevation of the residual topography. Only the youngest portion of the Réunion chain is shown in the main map. The two insets show the two separate geometric constraints for the entire chain (dashed red box area), as used in our modelling. Only chains RE, TR, ST and CN were used to determine the models, with other chains used for validation.

will honour the Mascarene Plateau geometry and the other (model B) will honour the Chagos-Laccadive chain on the India Plate; (4) The northern trend of the Walvis Ridge around 80 Ma is the earliest recorded change in Africa APM reflected in the hotspot chains, indicating a change in the location of the Euler pole (O'Connor & Le Roex 1992). The hotspot trail of the only other long-lived hotspot chain, St. Helena, is obscured by Cameroon Line volcanism, so plate motion past this time frame would have to incorporate hotspot trails from neighbouring plates using relative plate motions (e.g. Müller *et al.* 1993). Consequently, this study will limit itself to the kinematics after ~80 Ma.

With these features and modelling compromises in mind we will model the Africa APM using the hybrid Polygon Finite Rotation Method (PFRM) of Wessel *et al.* (2006). First, we review the data sets used in this endeavour.

5 DATA CONSTRAINTS

5.1 Geometric data

Initially, the topography of the hotspot chains on the Africa Plate was isolated from other features. Using the ETOPO2 global relief grid, the background seafloor elevation was removed using a spatial median filter with a diameter of 700 km (based on trial and error). To eliminate anomalies that were less pronounced in height, such as mid-ocean ridges and fracture zone fabric, an elevation cut-off of 700 m was applied. Thus, bathymetric features with a background seafloor corrected height below 700 m were not considered to be part of the hotspot chain. Other features that were not caused by hotspot volcanism were removed manually by enclosing each hotspot chain in a polygonal envelope. Any feature outside the envelope is not considered part of the volcanic hotspot chain. This partitioning allows continental features within a chain (e.g. the Seychelles), volcanism that does not describe the geometry of the main hotspot path (e.g. Rodrigues Ridge, Selvagem Islands), or features associated with fracture zone tracks (e.g. those crossing the St. Helena chain) to be removed in order to clarify the hotspot trail signals (Fig. 3).

5.2 Age data

Dated seamounts on the Africa Plate were used to determine how the plate moved in time; the sample distribution is shown in Fig. 1. Whenever possible, $^{40}Ar/^{39}Ar$ isochron ages were used as model constraints because they are typically more robust. Isochron ages were selected if the $^{40}Ar/^{36}Ar$ ratio was greater than or equal to 295.5 within its given uncertainties (Koppers *et al.* 2012), and $^{40}Ar/^{39}Ar$ plateau ages were used if the ratio was below that value. Because of limited $^{40}Ar/^{39}Ar$ data, K/Ar ages from the Canary chain were also incorporated into the model, and other dating techniques were used for specific drill hole sites (Table 2). In general, age data are limited and poorly distributed along the hotspot trails. To compensate, both age and age uncertainty grids were interpolated from the known ages and their uncertainties using a spline-based approach. Thus, for any given position along a trail we obtain an expected age and its uncertainty (Fig. 4).

Table 2. Age dated samples used for model constraints.

Sample	Lon (E°)	Lat (°N)	Age (Myr)	± (Myr)	Comments	Citations (age, location)
			Réunion			
Piton de Fournaise	55.71	− 21.24	2.1	0.3	Active volcanism, oldest age on Réunion Island is K-Ar	1, Piton de Fournaise
Mauritius	57.47	− 20.4	7.5	0.5	Isochron age, original shield volcano is 7–8 Myr	2, Piton de la Petite Riviere Noire
NB-1	60.3	− 15.0	31.5	0.3	Isochron age	2, 3
SM-1	60.0	− 9.5	47.5	3.6	Isochron age	2, 3
ODP 115–706	61.37	− 13.11	32.9	0.7	Isochron age	2, 4
ODP 115–707	59.02	− 7.55	64.1	1.1	Isochron age	2, 4
ODP 115–713	63.57	− 11.64	49.6	.06	Rotated from Chagos-Laccadive Ridge using Müller *et al.* (2008) rotations (model A)	
			Chagos-Laccadive Ridge			
ODP 115–713	73.39	− 4.19	49.6	0.6	Isochron age	2, 4
ODP 115–715	73.83	5.08	57.5	2.5	Isochron age	2, 4
DSDP 238	70.53	− 11.15	36	2	34–38 Ma	5, 5
Deccan	71.8	17.92	64.7	0.6	Location was moved west to correspond with the hotspot track	6, Mahabaleshwar
			Tristan-Walvis			
CH19 DR3–2	9.33	− 19.37	114.1	0.2	Plateau age, weighted mean	7, 7
CH19 DR3–22	9.33	− 19.37	108.3	0.4	Plateau age, weighted mean	7, 7
CH19 DR4–1	9.02	− 19.85	112.8	0.45	Plateau age	7, 7
CH19 DR4–2	9.02	− 19.85	112.4	0.55	Plateau age	7, 7
CH19 DR4–3	9.02	− 19.85	112.6	0.4	Plateau age	7, 7
DSDP Leg 74- 525A-57–2	2.99	− 29.07	71.3	0.4	Plateau age, weighted mean	7, 7
DSDP Leg 74- 525A-57–5	2.99	− 29.07	72.0	0.6	Plateau age	7, 7
DSDP Leg 74- 528–43–2	2.32	− 28.53	66.9	1.95	Plateau age	7, 7
AII-93–5–3	− 5.03	− 34.29	36.1	0.5	Plateau age	7, 7
AII-93–6–1	− 4.98	− 34.35	33.4	0.5	Plateau age	7, 7
AK-1695–6	− 7.73	− 36.42	27.0	0.05	Plateau age	7, 7
420–1-DR21–1	2.55	− 32.79	47.0	0.1	Plateau age	7, 7
423–1-DR25–4	0.55	− 34.93	45.6	0.05	Plateau age	7, 7
AII-93–10–11	− 1.57	− 34.34	49.4	0.35	Plateau age	7, 7
PS69/440–1-DR32–2	− 2.43	− 37.48	37.1	0.1	Plateau age	7, 7
PS69/440–1-DR32–5b	− 2.43	− 37.48	36.9	0.1	Plateau age	7, 7
AII-93–3–1	− 7.78	− 37.1	28.4	0.6	Isochron age	8, 8
AII-93–3–25	− 7.78	− 37.1	30.8	0.4	Isochron age	8, 8
AII-93–7–1	− 3.63	− 34.5	38	0.2	Isochron age	8, 8
AII-93–8–11	− 3.48	− 34.5	35.6	0.3	Isochron age	8, 8
AII-93–11–8	− 0.02	− 32.97	62	1.3	Isochron age	8, 8
V29–9–1	1.12	− 32.63	50	7.1	Isochron age	8, 8
AII-93–14–1	2.39	− 31.99	60.2	1	Isochron age	8, 8
AII-93–14–19	2.39	− 31.99	59.9	2	Isochron age	8, 8
DSDP 74–528–40–5	2.32	− 28.53	79.1	6.3	Isochron age	8, 8
AG51–2–1	− 12.28	− 37.12	0.64	0.3	Isochron age	9, 9
AG51–7–1	− 8.55	− 40.17	8.1	0.8	Isochron age	9, 9
AG51–9–1	− 6.22	− 39.47	18.7	0.2	Isochron age	9, 9
			St. Helena			
AC-D-02H	4.77	− 2.32	80.2	0.4	Plateau age	9, 9
AC-D-05A	4.47	− 4.28	77.5	0.4	Plateau age, 4 28′7″ W used instead of E	9, 9
AC-D-06	1.55	− 8.42	52.3	0.3	Plateau age	9, 9
AC-D-02E	4.77	− 2.32	79	0.9	Isochron age	9, 9
AC-D-02B	4.77	− 2.32	80.1	1.3	Isochron age	9, 9
SO84 43DS-1 (Kutzov)	− 8.35	− 15.14	10.3	0.3	Isochron age	10, 10
SO84 53DS-1 (Benjamin)	− 8.52	− 16.2	7.5	0.5	Isochron age	10, 10
SO84 60DS-2 (Josaphine)	− 9.01	− 16.27	2.6	0.3	Isochron age	10, 10
SO84 68DS-1 (Bonaparte)	− 7.1	− 15.6	15.3	1.1	Isochron age	10, 10
SO84 68DS-2 (Bonaparte)	− 7.1	− 15.6	15.1	0.03	Isochron age	10, 10
SO84 68DS-5 (Bonaparte)	− 7.1	− 15.6	14.9	0.1	Isochron age	10, 10

Table 2 (*Continued.*)

Sample	Lon (E°)	Lat (°N)	Age (Myr)	± (Myr)	Comments	Citations (age, location)
SO84 68DS-6 (Bonaparte)	– 7.1	– 15.6	14.2	0.6	Isochron age	10, 10
SO84 69DS-2 (Bonaparte)	– 6.95	– 15.8	14.5	0.5	Isochron age	10, 10
M16/1–6 (Bonaparte)	– 7.01	– 15.64	15.1	0.2	Isochron age	10, 10
SO84 71DS-6 (Bagration)	– 6.56	– 15.38	17.9	0.3	Isochron age	10, 10
SO84 72DS-2 (Bagration)	– 6.49	– 15.41	18	0.5	Isochron age	10, 10
SO84 73DS-1 (Bagration)	– 6.47	– 15.42	18.8	0.2	Isochron age	10, 10
SO84 74DS-1 (Bagration)	– 6.46	– 15.44	18.9	0.3	Isochron age	10, 10
			Canary			
DS 822–4 (Conception)	– 12.66	29.82	16.8	1.4	Isochron age	11, 11
DS 822–2 (Conception)	– 12.66	29.82	18.1	3.2	Isochron age	11, 11
Lars	– 13.29	32.8	68.2	2	Isochron age	11, 11
Tenerife	– 16.61	28.27	11.29	0.24	Isochron age, oldest reported age	12, Tenerife Island
Hierro	– 18	27.75	1.12	0.02	K-Ar age, oldest reported age	13, Hierro Island
La Palma	– 17.87	28.67	2	0.1	K-Ar age, oldest reported age	14, La Palma Island
Gomera	– 17.13	28.1	15.5	1.3	K-Ar age, oldest reported age	15, Gomera Island
Gran Canaria	– 15.6	27.97	14.64	0.29	K-Ar age, oldest reported age	16, Gran Canaria Island
Fuerteventura	– 14.02	28.33	20.4	0.4	K-Ar age	17, Fuerteventura Island
Lanzarote	– 13.63	29.04	15.5	0.3	K-Ar age	17, Lanzarote Island

References: 1, (McDougall 1971); 2, (Duncan & Hargraves 1990); 3, (Meyerhoff & Kamen-Kaye 1981); 4, (Vandamme & Courtillot 1990); 5, Purdy & Bertram (1993); 6, (Chenet *et al.* 2007); 7, (Rohde *et al.* 2013); 8, (O'Connor & Duncan 1990); 9, (O'Connor & Le Roex 1992); 10, (O'Connor *et al.* 1999); 11, (Geldmacher *et al.* 2001); 12, (Thirlwall *et al.* 2000); 13, (Guillou *et al.* 1996); 14, (Ancochea *et al.* 1994); 15, (Cantagrel *et al.* 1984); 16, (Guillou *et al.* 2004); 17, (Coello *et al.* 1992).

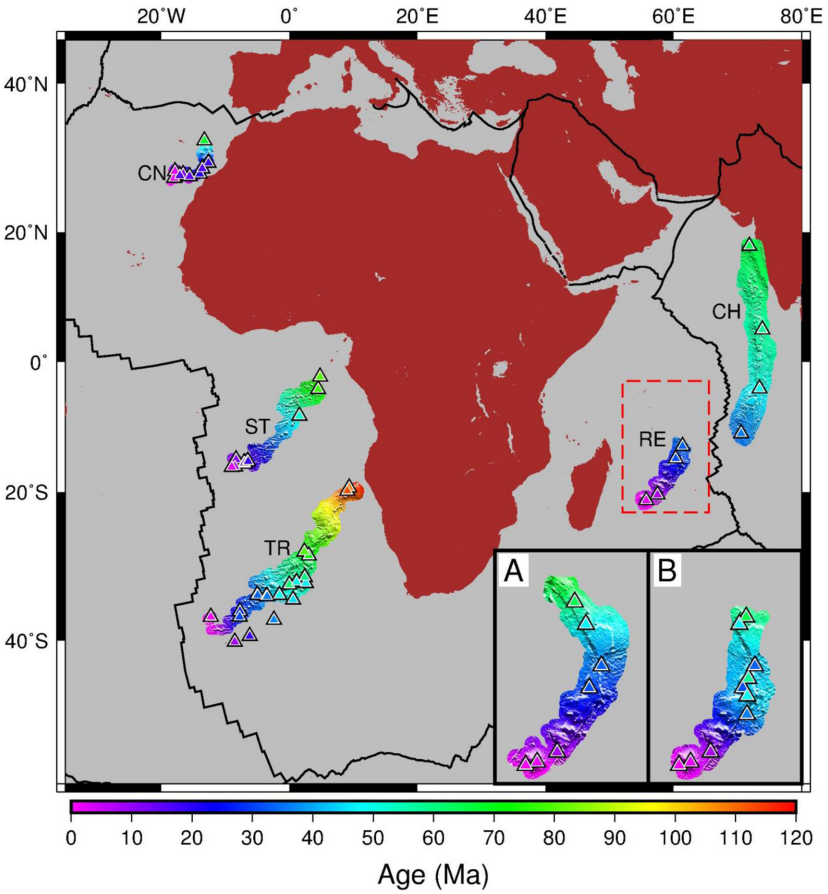

Figure 4. Extrapolated age map. Dated seamounts are shown as color-coded triangles, along with the spline-extrapolated ages for any given point along the residual grid of the four hotspot trails used for fitting. As with the geometric constraints, the age grid for Réunion chain was prepared differently for modelling the Mascarene Plateau (A) or the Chagos-Laccadive Ridge (B).

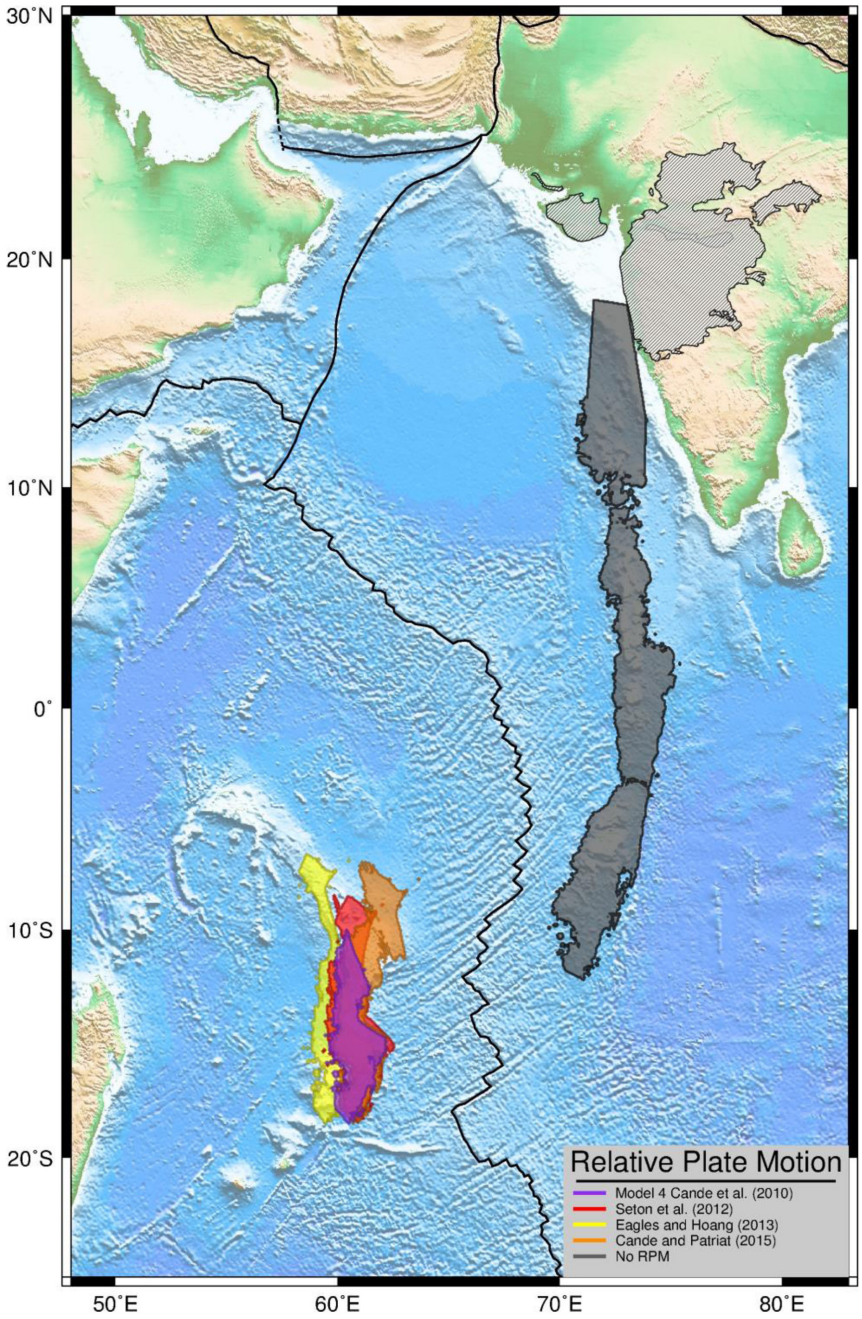

Figure 5. Reconstructing the Chagos-Laccadive Ridge onto the Africa Plate. Using India-Africa RPMs from Cande *et al.* (2010), Seton *et al.* (2012), Eagles & Hoang (2013), and Cande & Patriat (2015) yields slightly separate reconstructions of what a Réunion trail would look like if the Africa Plate had extended further north to capture the volcanism related to the hotspot. Hachured area denotes the Deccan Traps.

5.3 Extending the Réunion trail

While model A will derive entirely from data presently on the Africa Plate, model B depends on taking the geometry and age progression of the Chagos-Laccadive trail on the India Plate and rotating these into the Africa reference frame using a suitable set of RPM rotations for the India–Africa motion across the Carlsberg Ridge. Several RPM models have been proposed for this plate boundary; hence we explore some of the variability in the reconstruction by trying different models. Fig. 5 shows our interpretation of the extent of the Chagos-Laccadive Ridge and its reconstruction onto the Africa Plate. The colour-coded polygons represent the different reconstructions using three different published RPM models. Depending on the model chosen, the corresponding polygon data (and rotated age samples) will be combined with the younger portion of the Réunion chain, resulting in an interpretation of the longer and continuous Réunion hotspot trail that would have been observed if the Carlsberg Ridge were not present and the Africa Plate had captured all the outpouring from the Réunion plume.

6 METHODS

The method for determining a new Africa APM model closely follows the hybrid Polygonal Finite Rotation Method (PFRM, Wessel *et al.* 2006; Wessel & Kroenke 2008), with a few modifications

Table 3. List of hotspot locations.

Name	Lon	Lat	Used for fit	Radius (km)	Start time (Ma)
Réunion	54.7	− 21.5	Yes	70	67
Tristan	− 12	− 38.5	Yes	60	129
St. Helena	− 8.5	− 16	Yes	80	80
Canary	− 17.25	28	Yes	60	67
Cape Verde	− 25	15	No	75	26
Madeira	− 17.3	32.6	No	75	76
Shona	0	− 51.6	No	75	44
Discovery	− 4.7	− 45	No	75	44
Bathymetrist	− 28	4	No	75	58
Great Meteor	− 28.5	30	No	75	80

to account for circumstances that are unique to the Africa Plate motion. With residual topography of the hotspot chains specified, their associated hotspot positions are used to determine all compatible rotations. The present zero-age locations for the selected hotspots are not known but are presumably close to the youngest dated features. A given opening angle is tested over a full range of rotation pole locations. Each rotation that reconstructs the hotspot on or within a given distance threshold of its associated chain is considered a 'hit' and recorded, with preference given to rotations that fit the largest number of chains simultaneously. Given this subset of successful rotations, quaternion filtering is used to find smoothed rotation poles as a function of rotation angle, yielding an ideal geometric model. Given the finding of O'Neill *et al.* (2005) that hotspot motion proved insignificant at time periods since 80 Ma, fixed hotspot locations were used. Any systematic mismatch between the model and the data is likely to reflect this assumption. The PRFM method uses trial-and-error to examine the effect of perturbing the zero-age locations in order to determine improved locations that yield the most complete geometric model. While this approach addresses first-order adjustments between initial and final (Table 3) hotspot locations, we hope future modeling efforts can incorporate a more exhaustive search.

Two APM models were created based on two different interpretations of the Réunion hotspot trail: one that satisfies the geometry and age progression inferred for the Mascarene Plateau (model A), and one that instead fits the Chagos-Laccadive trail after its geometry and age samples were reconstructed (using India–Africa relative plate motions) onto the Africa Plate to join the Réunion hotspot track (model B). The two data sets for the Réunion hotspot trail(s) are shown in insets A and B in both Figs 3 and 4.

6.1 Mascarene Plateau Fit (Model A)

In this model, the residual grid of the Réunion hotspot track consisted of commonly attributed features from Réunion Island to the Nazareth Bank, but also included the more northerly features of the Saya de Malha Bank and Mascarene Plateau, assuming these volcanic features reflect a change in plate motion related to a chron 21 event. This is clearly the more speculative model of the two. To highlight the key requirements in fitting the Réunion-Mascarene Plateau trail we have created an approximate 4-stage model to explore what the implications are for the Africa Plate when these geometric features are satisfactorily modelled, and then use those insights to guide the actual PFRM modelling.

Therefore, from 0 to 20 Ma (Stage A), the key objective was to match the youngest trend of the Canary chain and the southwest portion of the Réunion chain as closely as possible, while simultaneously honouring the age progressions and geometries of the other chains. This was accomplished by drawing a great circle from the current hotspot position to a point along the chains approximately dated at 20 Ma for both the Réunion and Canary chains. Bisectors for both lines were constructed, and the pole for this stage rotation is located at the intersection of the two bisectors. These conditions imply an Euler pole close to the Canary chain (Fig. 6a), which results in a satisfactory fit to all the chains.

From 20 to 50 Ma, Stage B replicates the trend of the Réunion hotspot chain up to the Saya de Malha Bank while simultaneously predicting a Canary hotspot trail with a more distinct north–south orientation. Using the same procedure as for Stage A, the bisectors of the representative lines for the Canary and Réunion chains from 20 to 50 Ma were found, and their crossing indicated the location of a suitable stage pole. These conditions produce a stage rotation that has good agreement among the other hotspot chains as well (Fig. 6b).

Stage C (50–67 Ma) was modelled using two different approaches, both assuming that a stationary Réunion hotspot produced the Mascarene Plateau during this time interval. Since the trail segment for this stage is difficult to delineate in other chains (for reasons that will become clearer later), we only have a single bisector: a median line was constructed through the Mascarene Plateau and a single-stage rotation pole was assumed to be located somewhere along its bisector. If the rotation pole along the bisector were placed slightly east of the Tristan chain, then reversals in several Atlantic hotspot trails would be predicted (Fig. 6c, part 1). However, if it were located to the west of the chain, then no reversal but a sideways jog would be predicted (Fig. 6c, part 2). A potential reversal in the hotspot trail has interesting implications along the Tristan chain because it could potentially explain some of the large age reversals that have been observed along the Walvis Ridge mid-section as well as the puzzling bifurcation of the chain itself. Certainly, if this model reflects Africa motion during this interval then none of the Atlantic-side trails could clearly display it. Finally, stage D is a continuation of the model from 67 to 80 Ma. Here we fit the St. Helena and Tristan chains only, as no other chains on the Africa Plate itself are older than ∼70 Ma (Fig. 6d). These initial sketches guided our work with the hybrid PFRM.

Initial PFRM results revealed rotations that successfully reconstructed points along the Mascarene Plateau onto the Réunion hotspot (the desired rotations are therefore the transpose rotations). However, these rotations exhibited a very limited range of opening angles, not differing by more than one degree or less. In fact, we found that the rotation pole locations were moving considerably

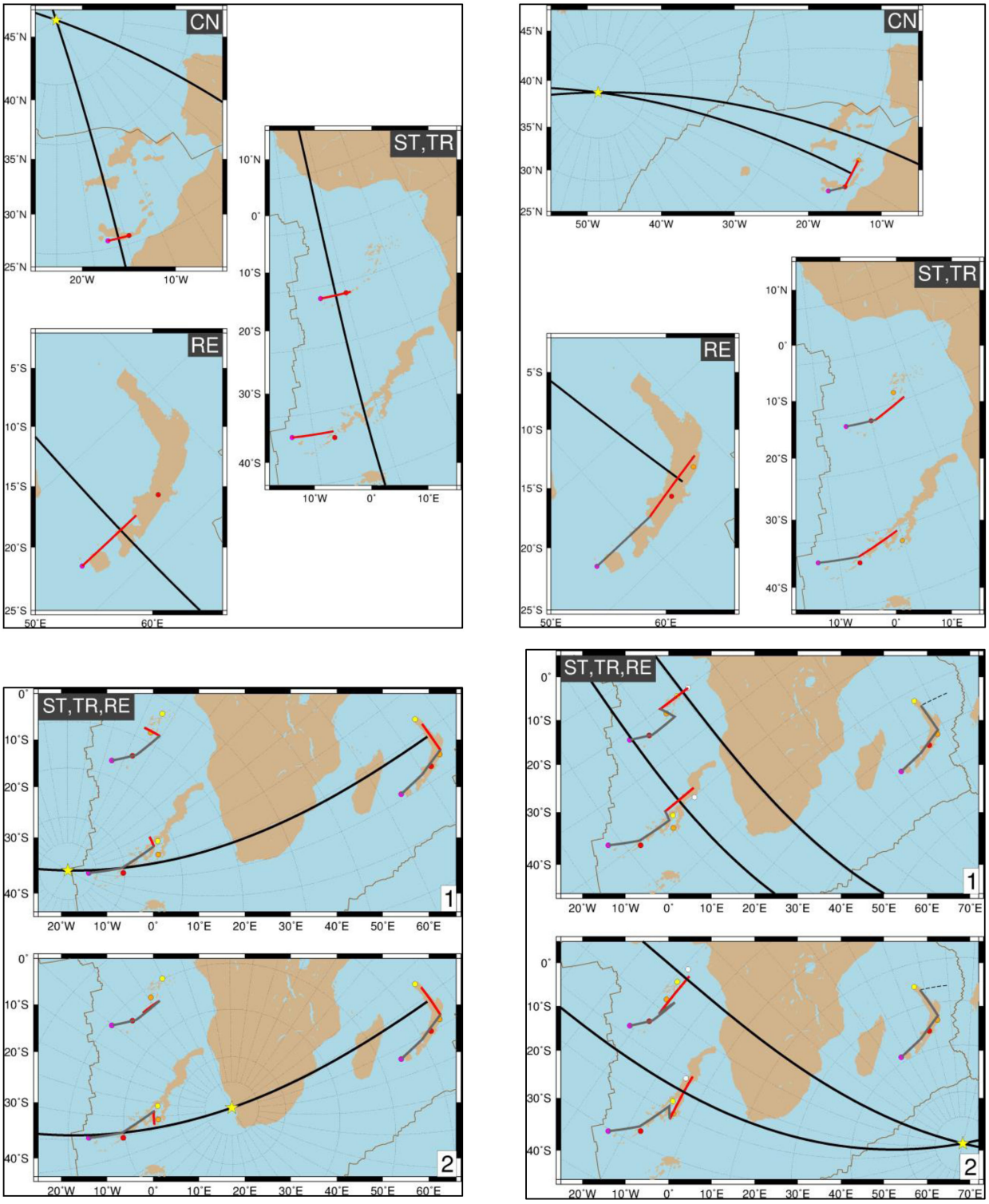

Figure 6. Preliminary 4-stage sketch model A for Africa APM. Solid black lines are bisectors between for key stages of each trail. The resulting stage trail segment is shown as a red line, while previous stages are drawn in grey. Oblique gridlines about the Euler pole (yellow star marking bisector intersection) are shown as dotted lines. (a) Stage A model for Canary, Réunion, Tristan and St. Helena, using bisectors between hotspot location and a tentative ~20 Ma point. (b) Stage B model for Canary, Réunion, and Tristan and St. Helena determining the bisectors between a ~20 Ma and a ~50 Ma point (orange circle) on the Réunion hotspot track. (c) Stage C model for the Tristan chain. The bisector is for the segment between a ~50 Ma point (orange circle) and a ~67 Ma point (yellow circle) on the speculative Mascarene Plateau of the Réunion hotspot track. A single-stage rotation pole was assumed to be located somewhere along its bisector. If a rotation pole (yellow star) is selected to the west of the Tristan chain no reversal occurs along the hotspot track (1), but if a pole between Tristan and Africa was chosen the trail would experience a reversal along the Tristan chain (2). (d) Stage D model for Tristan, Réunion and St. Helena chains, with a reversal (1) and without a reversal (2) inherited from stage C. The bisectors are for the segment between a ~67 Ma point (yellow circle) and an ~80 Ma point (white circle) on each of the Tristan and St. Helena chains.

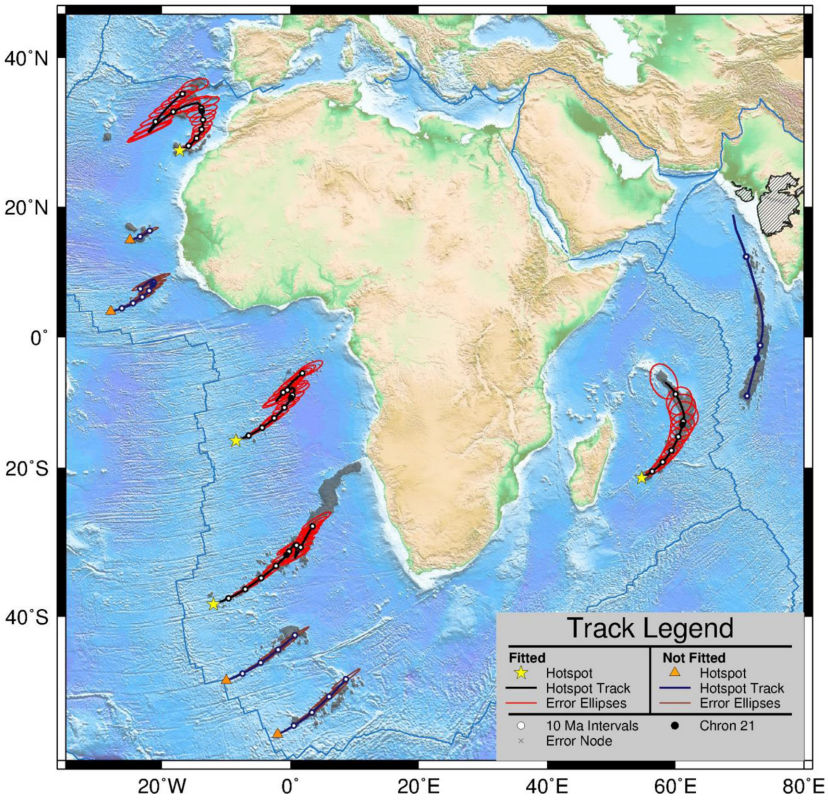

Figure 7. Africa APM model A (Mascarene Plateau fit). Solid line shows model trail predictions, with white circles every 10 Myr. Select error ellipses (red) are shown for readability. Hachured area denotes the Deccan Traps. See legend for more details. See Supporting Information for the complete listing of model parameters.

while the rotation angles remained nearly constant. In its geometric analysis, the Hybrid PFRM of Wessel *et al.* (2006) uses opening angles as a proxy for ages, so the method breaks down when the angle is not monotonically increasing along a hotspot trail. Consequently, the smoothing of rotations as a function of angle ended up averaging all these different pole locations, yielding a single, meaningless rotation. Hence, increasing angle could not be used as a proxy for age for this section, and a new proxy had to be found. In the simplest terms, increasing distance from the hotspot indicates older hotspot material, so distance along the Réunion trail was explored as a proxy for age.

In order to test our model A hypothesis, we wanted to focus on rotations that yielded acceptable results along the Réunion hotspot chain, being the most focused chain. A median line was determined through the entirety of the chain to guide the filtering of the above rotations as a function of distance. At 50 km intervals along this line, all reconstructed points ('hits') that fell within a circle of 100 km radius of that position were found. Then, the rotations responsible for these reconstructed points were filtered to find an average rotation pole and opening angle for each circle. This procedure yielded a set of rotations that fit the entirety of the Réunion hotspot chain up through the Mascarene Plateau while still honouring the other three chains included in the modelling. Our final set of rotations for model A predicts reversals along several hotspot chains on the western side of Africa (Fig. 7) similar to that of our exploratory stage model (Fig. 6c). In fact, stage rotation poles for the 67–50 Ma interval all lie near southern Africa.

Since we were testing the hypothesis that the chron 21 and 29/30 changes seen in the seafloor fabric corresponded to the Réunion bend and initiation of the Deccan Traps, respectively, we chose to interpolate and extrapolate the limited ages for this interval to satisfy those boundary conditions. This led to an age-distance relationship that was used to determine the APM model up to the terminus of the Réunion chain at ~65 Ma. With only the St. Helena and Tristan chain used for further analysis beyond 67 Ma, a stage pole was appended from 67 to ~80 Ma that fit both the Tristan and St. Helena chains while minimizing the change in plate velocity. The final model was then smoothed with REDBACK to reduce plate tectonic noise in the reconstruction (Iaffaldano *et al.* 2014). Because REDBACK smoothing is sensitive to window widths and other parameters we considered both the initial and smoothed models in our analysis (see supplementary material for all models).

6.2 Fitting the rotated Chagos-Laccadive Ridge (Model B)

Another interpretation of the Réunion hotspot trail states that no part of the Mascarene Plateau was caused by Réunion hotspot volcanism, but instead was a result of rifting and flank volcanism following spreading in the Mascarene Basin. This interpretation considers the Chagos-Laccadive chain on the India Plate a continuation of the Réunion chain. The geometry of this trail was first reconstructed into the Africa reference frame using its interpolated age grid and India-Africa relative plate motions, which lead to partial overlap with the Réunion hotspot trail. The final model B is sensitive to the selection of India–Africa relative motion. Hence, several published India–Africa RPM models were explored and found to yield different reconstructions; the Seton *et al.* (2012) RPM was chosen for our fit as it was representative of all the reconstructions (red polygon in Fig. 5). The Chagos-Laccadive age data were also rotated

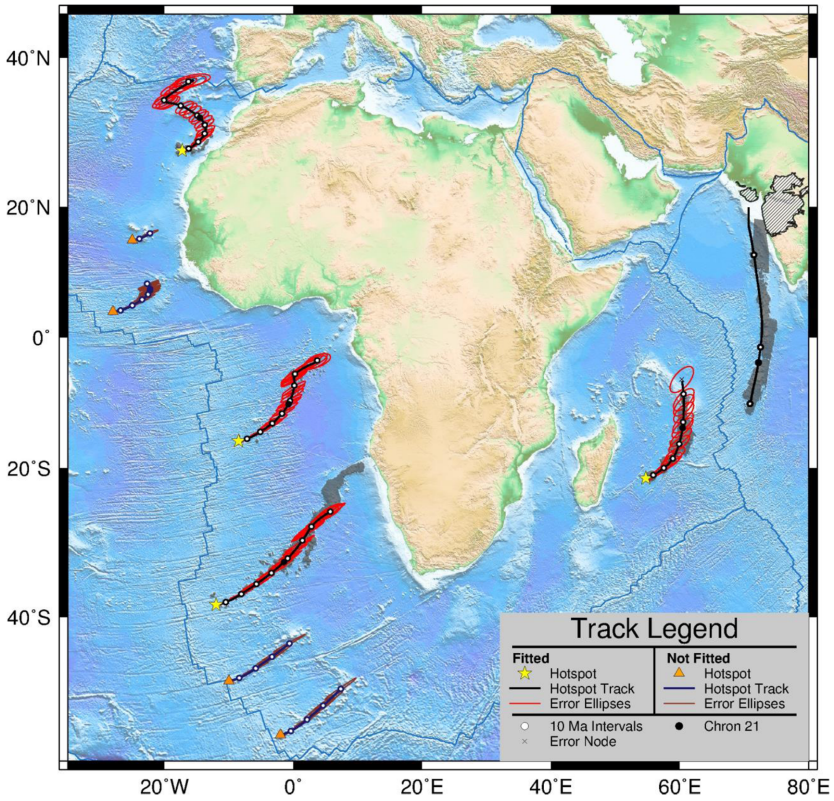

Figure 8. Africa APM model B (Chagos-Laccadive fit). Solid line shows model trail predictions, with white circles every 10 Myr. Select error ellipses (red) are shown for readability. Hachured area denotes the Deccan Traps. See legend for more details. See Supplementary Materials for the complete listing of model parameters.

into the Africa reference frame and splined with Réunion ages to yield an alternative age grid for the Réunion hotspot track (Fig. 4; insert B). The standard hybrid PFRM was used to produce the initial raw model. As for model A, the final model B (Fig. 8) was then obtained by smoothing the raw model with REDBACK (Iaffaldano *et al.* 2014).

7 DISCUSSION

7.1 Geometric analysis of models A and B

Our two models share many common features, in particular for the youngest 50 Myr, but depart considerably from each other during the key 50–67 Ma interval. Here, model A by design fits the Mascarene Plateau, and it is this condition that produces the reversals predicted for several of the Atlantic Ocean trails as well as the near-pivoting of the Africa Plate. Fig. 9 shows this pivoting as a general clustering of 50–67 Ma stage poles near the 50–67 Ma (stage C) sketch stage pole (star) from Fig. 6c. Prior to 67 Ma the two models are again largely similar. Model B, by taking a gentler turn at chron 21, predicts no such reversals, thus failing to satisfy some of the data constraints on the plate itself, such as the observed 10+ Myr age reversals in the Walvis chain and the double-trail geometry in this area. However, it is of course not possible to determine if the inferred reversals actually reflect plate motion or instead are variability in the surface expression of this particular plume-plate interaction without finer sampling of the hotspot trails. Model B thus remains a viable geometric solution. For model B, the 50–67 Ma stage poles cluster near Brazil, off the Africa Plate itself, and approach the stage poles of Cande & Stegman (2011). We notice that the reconstruction of the Chagos-Laccadive Ridge onto the Africa Plate (Fig. 5) is relatively sensitive to the RPM model used. While our primary source of rotations for this study is the RPM compilation of Seton *et al.* (2012), we note that the India–Africa rotations of Eagles & Hoang (2013) lead to a reconstruction more aligned with the Mascarene Plateau. The same paper also describes the anticlockwise motion of the Seychelles Plate relative to Africa before 59 Ma, which would cause the severity of the bend to be overestimated. If this rotation were undone, it would decrease the bend in model A and potentially resolve some of the differences in geometry between the models. Clearly, more testing of alternative Chagos-Laccadive reconstruction scenarios will be required to map the continuum of possible models between A and B to see if an optimal model can be determined.

Both models extend the Canary trail prediction up through the Madeiras, thus providing an explanation for older samples with distinct Canary plume signatures within/beneath the younger Madeiras edifice. The gap in volcanism between the end of the Canary chain and the start of the (old portion of the) Madeiras seems to correlate with a rapid increase in predicted plate velocities for this area, preventing the impinging plume from penetrating the thick plate to produce surface volcanism; this is particularly true for model A.

7.2 Comparison to previous models

Generally, model B predicts hotspot trails similar to previous APM models, while model A is a more alternative interpretation. The Duncan & Richards (1991) model does not seem to be able to replicate the St. Helena and Tristan hotspot tracks with much accuracy, but that is most likely due to our estimates of their hotspot positions

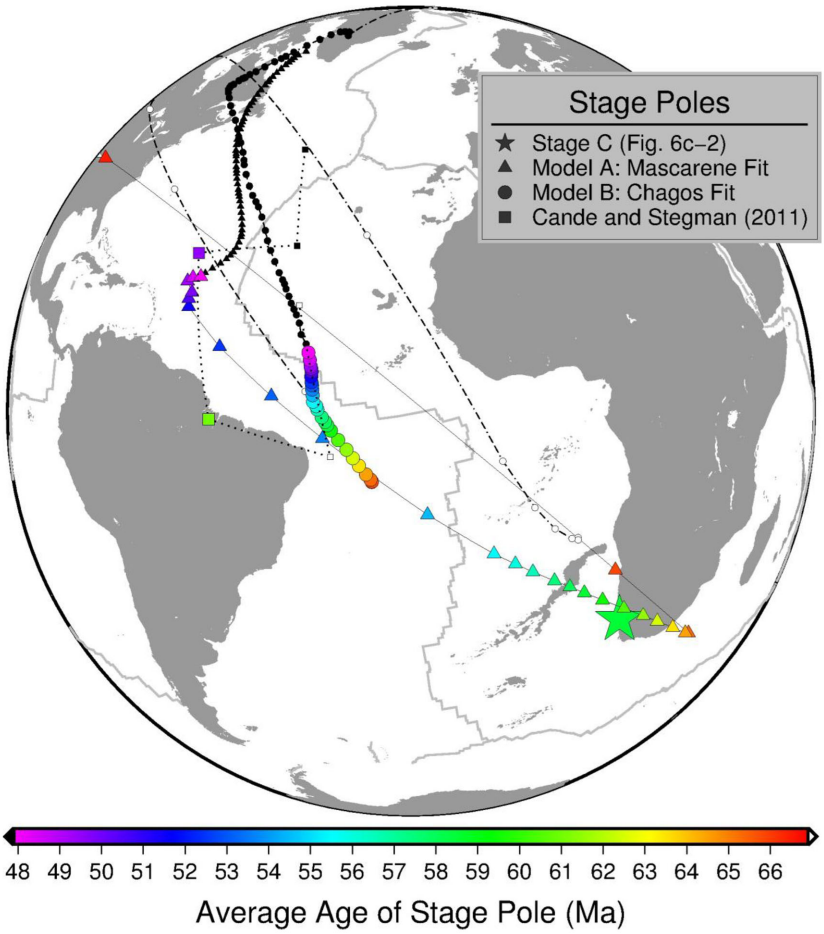

Figure 9. Location of stage poles for model A (triangles), B (circles), the Africa APM (squares) of Cande & Stegman (2011) and stage C (47–50 Ma) of our 4-stage sketch (star). Lines show the path of stage poles progression. Open and solid symbols are stage poles before and after the highlighted time interval, respectively. Only rotations within the 50–67 Ma interval have been color-coded. Model A reflect the insight from our 4-stage model, showing pivoting of Africa around points near South Africa, while model B also pivot but these poles are just outside the Africa Plate in the Equatorial Atlantic and more similar to the model by Cande & Stegman (2011), which again depends on the Antarctica APM of Müller *et al.* (1993).

from their illustrations; the trend of the trails is otherwise similar (Fig. 2b). Their fit to the Cape Verde hotspot is better than our revised model, but fitting it has created artefacts along the Canary hotspot trail, creating a sharp bend when no bend is present. Their model also indicates a departure from the Réunion hotspot trail at the northern end of the Nazareth Bank at 36 Ma. This means our models more smoothly replicate these trails, and follow the Canary shape more accurately.

There are many similarities between our new APMs and the Müller *et al.* (1993) model, particularly in the Réunion, St. Helena, and Tristan hotspot tracks. The Müller model does not predict the presence of seamounts in the northern part of the St. Helena chain and only follows the northern portion of the Tristan chain. Our new APMs predict much closer fits to the Canary hotspot chain, but they fail to follow the Great Meteor hotspot trail, where the Müller *et al.* (1993) model follows the path more closely. However, the possibility of ridge-hotspot interaction and a lack of age dates along the trail prevent a conclusive test.

The O'Neill *et al.* (2005) predicted hotspot tracks show many similarities to our new APM models for more recent times, though they are less smoothly rendered and suggest bends along the Tristan chain where there are none, including a southern-sweeping trend from 0 to 20 Ma to fit the Gough lineament. This is most likely due to the predicted motion of the Tristan hotspot from their mantle model during that time period. The Réunion track flows back to the Saya de Malha Bank at ~40 Ma, though the trend cuts into the Mascarene Basin where no volcanic features are seen. It is then projected on to the Chagos-Laccadive Ridge. On the St. Helena track, the hotspot trend is very similar until the 67–80 Ma mark, where it follows a more southern route through the seamount chain. The O'Neill *et al.* (2005) trend along the Great Meteor trail follows the residual topography of the chain closely. However, the large error ellipses render most of these discrepancies insignificant except for the Canary and St. Helena trails.

While the model of Cande & Stegman (2011) does an excellent job of fitting most of the key features, it fails when it comes to recreating the Canary bend. This underestimate of the bend is also reflected in the early stages of the Tristan chain, where it has taken a more southern route. At later stages it does fit both the St. Helena and Tristan chain, though the hotspot trail trends to the centre of the Tristan chain and ignores the bulk of seamounts on the northern lineament from chron 5r (10.4 Ma) to chron 18r (42.7 Ma).

The Doubrovine *et al.* (2012) model does not replicate what we see to be many of the key features on the Africa Plate, even when the confidence ellipses are considered. From 0 to 30 Ma, the

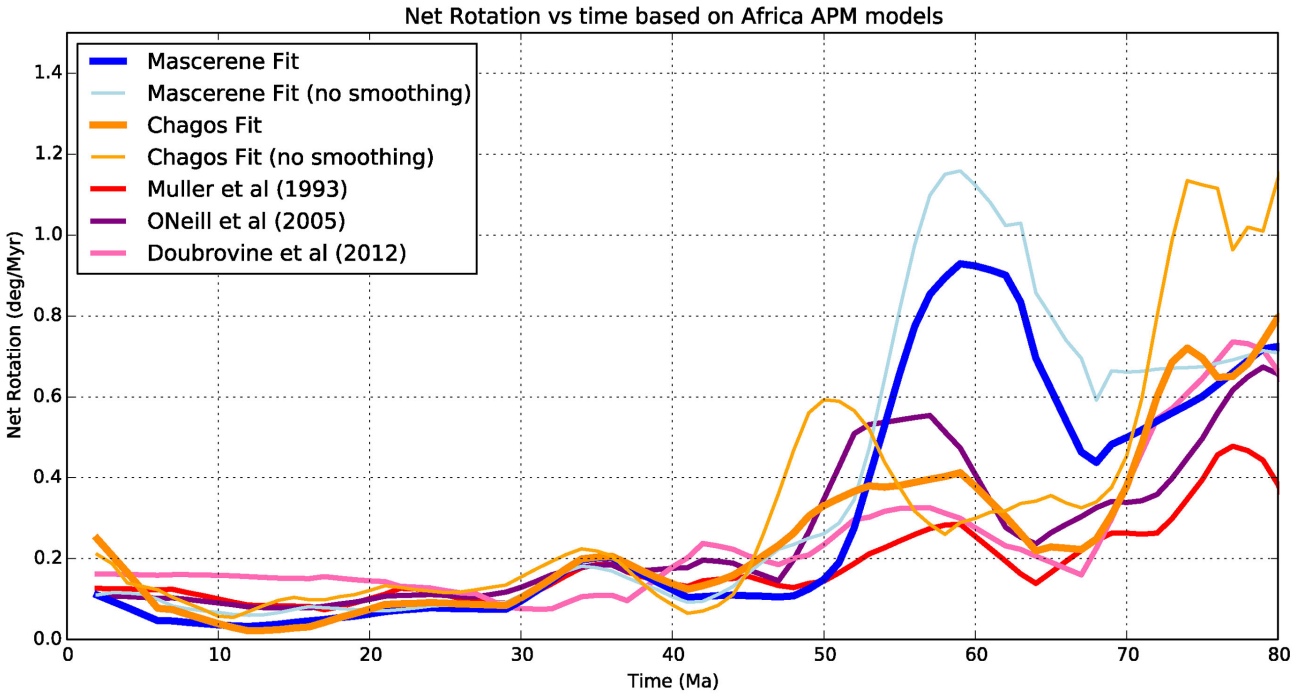

Figure 10. Net lithospheric rotations for various Africa APM models when combined with the global relative plate motion model of Seton *et al.* (2012) smoothed using a 5 Myr moving average. All models predict a general increase in NLR for times older than 50 Ma but differ in amplitudes and patterns. Model A exhibits a large excursion during the 67–50 Ma range. Model B has a large spike during the 80–70 Ma interval that is most likely an artefact from using just two chains (TR, ST) and hence limited age control.

predicted Canary trail curves in the opposite direction of its actual geometry, and the geometry of the hotspot trail along the Tristan and St. Helena hotspot chains suffers at later ages, moving away from the observed trail. Their predicted Réunion trail gives a reasonable fit until reaching the Saya de Malha Bank, where it is then projected to move eastward off the Chagos-Laccadive Ridge. However, their trail is predicted to be on the western side of the Réunion track rather than the middle.

7.3 Global net lithospheric rotation

APM models are an important component in estimates of net lithospheric rotation (NLR) through time (e.g. Torsvik *et al.* 2010). Using a combination of geodynamic modelling and seismological analysis, Conrad & Behn (2010) argued that NLR is unlikely to exceed 0.26° Myr^{-1}, but many reference frames yield larger values for some intervals in the last 100 Ma (Doubrovine *et al.* 2012). To investigate the implications of our APM results for NLR, we combined our APM models with RPM models that provide a continuous description of plate boundaries (Gurnis *et al.* 2012; Seton *et al.* 2012). We then calculated NLR at 1 Ma intervals, both for our APM models and the other comparable models (Fig. 10).

Predicted NLR for the Mascarene fit APM (model A) yields reasonable estimates of NLR from 50 Ma to present day, but the 50–70 Ma interval yields a period of much larger NLR, approaching 1° Myr^{-1}. Since Africa is the anchor plate for the global RPM model, major changes in the motion of Africa similarly affect the absolute motions of all other plates, and in this case yield a geodynamically unlikely scenario (see Fig. 11 for 60 Ma and Supplementary Materials for other times). Therefore, we must rule out the model A interpretation of the Africa APM. The Chagos fit (model B) produces reasonable NLR estimates for times earlier than 50 Ma, preceded by a ~10 Ma period of higher NLR (~0.4° Myr^{-1}), a signal also observed in other APM models and attributed either to the fast motion of the India Plate or the large overall motion of plates in the Pacific domain (Torsvik *et al.* 2010; Doubrovine *et al.* 2012). The fast velocities in the 67–50 Ma timeframe are also a function of the time constraints we imposed on the stage model. Should the start time prove to be earlier (e.g. 72–71 Ma) and end time be 48–47 Ma then our velocities may be in error by almost 50 per cent; this drop would have a considerable effect on net lithospheric rotations. Better age constraints will be needed to test these possibilities.

7.4 Model limitations

Many of the model limitations come from determinations of what physical indicators on the Africa Plate are truly attributable to plate motion. Obviously, the premise behind model A (e.g. that the Mascarene Ridge reflects Africa APM) appears to be wrong given the unreasonable NLR values a times earlier than 50 Ma, in which case the model is invalid. But even if the Mascarene Ridge hypothesis were valid, Palaeocene seafloor spreading in the Mascarene Basin might have continued until 59 Ma, and this delay would introduce systematic errors in model A. Addressing this bias would require us to retract a small amount of Mascarene Basin spreading which would probably make the Mascarene bend angle even larger and exacerbating the aforementioned net lithospheric rotation problems; hence, we have refrained from attempting this correction. The rotation of the Seychelles Plate would also affect the geometry of model A and cause the bend to be exaggerated. This requires further testing. Because of the Chagos-Laccadive trail reconstruction, model B is susceptible to uncertainties in models for Carlsberg Ridge spreading. Likewise, bias in our interpretation of the Chagos-Laccadive outline (Fig. 5) may also affect model B. Finally, hotspot or mantle

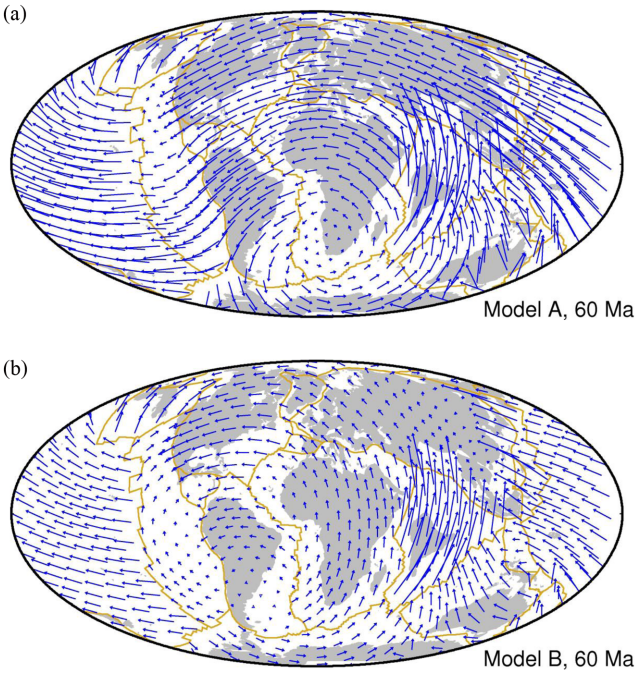

Figure 11. Global APM velocities at 60 Ma predicted for APM models when combined with the global relative plate motion model of Seton *et al.* (2012). (a) Model A (Mascarene fit) predicts a pivoting of Africa about a rotation pole in south Africa, implying fast velocities along its northern border that are not supported by local tectonics. (b) Model B (Chagos fit) reduces the pivoting by virtue of an equatorial rotation pole off the Africa Plate (see Fig. 9), producing lower APM velocities for other plates (and hence net lithospheric rotation overall). For APM velocities at different times, see Supplementary Materials.

motion, and recent Nubia–Somalia Plate motion could introduce systematic errors in both model A and B. Specifically, plate motion between Nubia and Somalia over the past 11 Ma would also bias the inferred rotations and may lead to errors of up to 100 km in the predictions of the Réunion and Chagos-Laccadive trails.

The Carlsberg Ridge also poses a problem for the exact positioning of the Réunion hotspot and the determination of the true hotspot track for both models. Conjugate magnetic anomalies around the ridge are progressively wider in separation, which is inconsistent with rotations that simultaneously fit the India, Capricorn and Somali plates at times earlier than chron 22o (Cande *et al.* 2010). Cande & Patriat (2015) have determined motion to chron 34y using 2-plate finite rotations, but the location of the Carlsberg Ridge is still not well constrained. The amount of time it spent over the Réunion hotspot is not known, and interactions between the plume and the ridge could have caused surface volcanism to form closer to the ridge axis instead of directly above the hotspot (Wessel & Kroenke 2009). If the Réunion hotspot was not situated below the Carlsberg Ridge from 67 Ma to chron 21, then it could not have concurrently formed the Mascarene Plateau and the Chagos-Laccadive Ridge, eliminating the possibility of our Mascarene fit model.

7.5 Implications for global plate motions

Though our Mascarene fit APM (model A) is inconsistent with accepted NLR estimates, it is instructive to compare it with with previous models during the ~45–65 Ma interval. The Africa Plate appears to stop its northeastward motion during the arrival of the Réunion plume head at the Deccan Traps at 67 Ma (Chenet *et al.* 2007). This corresponds with the inferred slowdown or pivoting of the Africa Plate proposed by Cande & Stegman (2011). This change in APM could also corroborate the idea of the Réunion plume push forcing Africa's change in motion, most likely accomplished by weakening the asthenosphere and thus making the combined ridge push and slab pull more efficient (Kumar *et al.* 2007; van Hinsbergen *et al.* 2011). During that time period, the Africa Plate appears to pivot as the total reconstruction pole moves in a more northwestern direction and the stage poles cluster near the approximate stage C pole (Fig. 9). The plate then resumes its general northeast motion around chron 21, possibly following the collision of India into Eurasia around chron 20 (Cande *et al.* 2010). In comparison, the Chagos-Laccadive fit (model B) is very similar to previous models and shows modest pivoting.

Despite their very different predictions for the Africa Plate, the projections of either Africa APM model via plate circuits into the Pacific fail to make an appreciable difference in the prediction of the Pacific APM (Fig. 12), and both are similar to that of other APM models projected into the Pacific. Previous work using the same circuit with prior Africa models have also failed to reproduce the Hawaii-Emperor chain (e.g. Raymond *et al.* 2000). The plate circuit we used was Africa–East Antarctica–West Antarctica–Pacific (Seton *et al.* 2012). In particular, neither model predicts any significant change of Pacific motion at HEB time. This behaviour mimics the Müller *et al.* (1993) and O'Neill *et al.* (2005) models but differs from the Doubrovine *et al.* (2012) model as the latter includes Pacific trails as constraints. The fixed Pacific hotspot WK08-A model of Wessel & Kroenke (2008) is shown for reference. It is not immediately obvious why an Africa APM chron 21 change would not manifest itself in the Pacific. Possible explanations involve the Antarctic Plate motion which is not well resolved between East and West Antarctica, and of course the possibility that there is no significant chron 21 event recorded around the Africa Plate. Other plate circuits may produce a slight bend without matching the actual bend (e.g. Steinberger *et al.* 2004). Additionally, the Africa Plate moves so slowly relative to the mantle that even a resolvable change in Africa Plate motion might not lead to significant changes when projected via the global plate circuit. It is noteworthy that even the large (and likely erroneous) APM change required for the Réunion-Mascarene bend (model A) projects to a gentle bend for the Chagos-Laccadive Ridge on the India Plate, hence a significant bend in the Pacific regime might not be expected.

7.6 Outlook

While these models offer a self-consistent explanation for many of the important features on the Africa Plate, several of the hypotheses require verification. The most important data to examine these hypotheses further would be an increase in the quantity and quality of age dating along the Réunion-Mascarene and Chagos-Laccadive trails. New geophysical and geochemical evidence along the Mascarene Plateau will be useful to test the hypothesis that it has a hotspot origin, and any age dating along the chain would help to identify the precise location of the chron 21 event along the chain and improve our age–angle relationship. This would help in determining which one of our contrasting models is more realistic.

In general, an increase in the number of dated seamount chains will help to constrain our model parameters, and $^{40}Ar/^{39}Ar$ dating along previously undated chains would allow them to be used to verify some of our model's claims. This would be particularly interesting along the Bathymetrist chain, where our Mascarene model

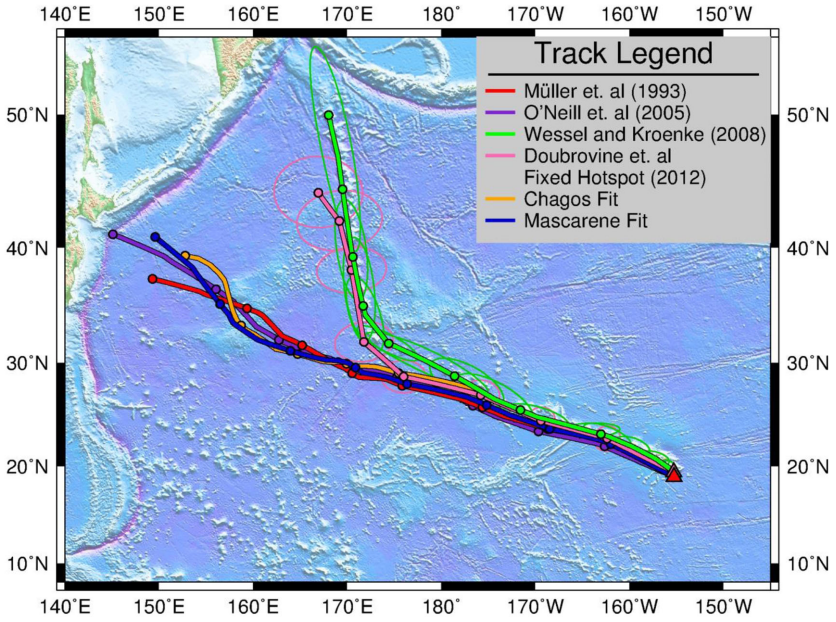

Figure 12. Trail predictions for the Hawaii-Emperor chain from Pacific and Africa-based APM models. Circles are placed every 10 Myr. Neither our model A nor B predictions, after projection via the Africa–East Antarctica–West Antarctica–Pacific Plate circuit, show any indication of a chron 21 bend.

predicts a hotspot trail reversal event similar to the one seen in the Tristan chain, so any age reversals that are observed would add validity to the Mascarene model. Furthermore, both our models imply that the Canary plume is responsible for the basal volcanism underlying the Madeiras, as suggested by Geldmacher *et al.* (2006); this connection could possibly be used to extend the Canary-Madeiras chain to the end of the plate boundary. Finally, better coverage of ages from both Tristan and St. Helena may be needed to confirm the age reversal predicted by model A.

Both models could possibly be improved by accommodating a small amount of hotspot motion, but we have refrained from doing so due to the relative lack of palaeomagnetic data from all four trails and the scarcity of age control. Furthermore, Indo-Atlantic plume drift is not expected to be large after ~80 Ma (O'Neill *et al.* 2005). Future work will seek to determine the simplest drift model compatible with all observations. Although our model successfully matches the Réunion-Mascarene trail, the possible presence of continental fragments along part of the chain requires further investigation. Finally, model A has unrealistically fast net rotation rates and predicts untenable APM velocities for other plates yet satisfies most of our other requirements. One possible explanation for this dilemma would be that our interpretation of Atlantic-side trail reversals is incorrect; thus model B is our preferred model. However, given the uncertainties in Africa–India RPM and seamount ages it remains possible that a model capable of explaining the inferred Africa Plate volcanic reversals while producing an acceptable net lithospheric rotation could be determined. We hope our two models may thus serve as a starting point for further discussion and modelling.

8 CONCLUSIONS

While observed changes in Africa's RPMs with neighbouring plates may allow for a synchronous change near chron 21, the evidence is not clear-cut and the exact timing is still being debated (e.g. Bernard & Munschy 2000; Cande *et al.* 2010; Cande & Patriat 2015). The dominant signal in Indo-Atlantic plate motions around chron 21 is India's rapid slowdown with respect to Africa (Cande & Patriat 2015); this event is more indicative of an APM change for India than for Africa. Seeking independent evidence from hotspot trail geometries and age progressions, we determined two Africa APM models using a modified version of the hybrid PFRM technique. We examined if (1) the Réunion hotspot formed the Mascarene Plateau as a part of this event, or if (2) it exclusively produced the Chagos-Laccadive Ridge on the India Plate during this time period.

First, we demonstrated it is geometrically possible to include the Mascarene Plateau as the continuation of the Réunion hotspot track (model A) while honouring the geometries of other hotspot chains. Model A predicts reversals in the Tristan and St. Helena hotspot tracks, which are consistent with Tristan-Walvis's bifurcation, observed age reversals along the Walvis Ridge, and perhaps the higher concentration of seamounts in the northern portion of the St. Helena chain. However, model A also implies unreasonably fast APMs for several neighbouring plates due to rapid pivoting during the 67–50 Ma interval about a high-latitude stage pole. These motions increase net lithospheric rotation by a factor of two relative to competing models, suggesting model A is geodynamically implausible.

Second, a more conventional model (B) instead fits the Chagos-Laccadive Ridge on the India Plate as a continuation of the Réunion hotspot track while omitting the Mascarene Plateau features on the Africa Plate northwest of the Nazareth Bank. Unlike model A, this model does not predict reversals in Atlantic hotspot trails. Model B shows a much more subdued pivoting of the Africa Plate during the 67–50 Ma interval given its equatorial stage poles close to South America, similar to the model of Cande & Stegman (2011). The APM velocities and net lithospheric rotations are more in line with previous models (Fig. 10). By ignoring the features we initially interpreted to reflect APM changes (i.e. Mascarene Bend and Walvis age reversals), this model predicts a subtler event near chron 21, or perhaps no significant event at all.

In both models, the Africa Plate is pivoting during the 67–50 Ma interval, but model A does so more extremely around stage poles near South Africa, whereas model B's equatorial stage poles yield lower velocities. Both models project the Canary hotspot track back

through the Madeiras, which agrees with ages and isotopic evidence of a Canary plume influence (Geldmacher *et al.* 2006). Neither model, when projected via a global plate circuit into the Pacific, can predict the HEB at chron 21, in agreement with other Africa-based APM models discussed earlier (Fig. 12), though a different plate circuit might change the projections somewhat (e.g. Steinberger *et al.* 2004). If there were a change in Africa APM at chron 21 it may simply have been too small to be reflected in the Pacific regime. Therefore, it seems clear that most of the HEB geometry reflects plume motion (Tarduno *et al.* 2009).

The distinct (and dated) bend in the Chagos-Laccadive Ridge reflects a chron 21 APM event for India and is well predicted by our models. For Africa itself, model B predicts much smaller changes, which do not lend strong support for a significant Africa APM change at chron 21. If such a change did occur, the evidence for it is presently buried below the noise threshold of our APM modelling. Thus at present, model B best represents Africa APM and other explanations will have to be pursued for the observed complications in the Tristan and St. Helena chains. Consequently, a global plate reorganization around 50 Ma remains best supported by RPM rather than APM models.

The dilemma of an Africa APM change at chron 21 may possibly be resolved with better data. First, we have shown that models for the motion across the Carlsberg Ridge (Fig. 5) differ considerably (Cande *et al.* 2010; Seton *et al.* 2012; Eagles & Wibisono 2013; Cande & Patriat 2015). Since we use such models to reconstruct the Chagos-Laccadive Ridge onto the Africa Plate, any bias in this reconstruction adds uncertainties to the magnitude and direction of the Africa APM around chron 21. A resolution of these RPM discrepancies would allow for a more robust Africa APM model. Secondly, the key hotspot trail observations that we interpreted to support an Africa APM change must be re-examined in more detail. In particular, better coverage of the Tristan chain (to resolve the nature of its apparent age reversals), the northern St. Helena chain (to confirm or rule out age reversals) and new samples from the Mascarene Plateau and the Réunion hotspot chain (to improve the observed age-progression and to assess the geochemical evidence for a hotspot connection) will likely be required. Given the importance of Africa to global plate motions we believe such data should be acquired.

ACKNOWLEDGEMENTS

Support for this work was provided for PW and SM by NSF grant OCE-106054. RDM and SEW were supported by Australian Research Council grant DP0987713 and Science Industry Endowment Fund grant RP04-174. We would also like to thank Graeme Eagles and an anonymous reviewer, whose comments greatly improved the paper. This is SOEST contribution 9300.

REFERENCES

Ancochea, E., Hernán, F., Cendrero, A., Cantagrel, J.M., Fúster, J.M., Ibarrola, E. & Coello, J., 1994. Constructive and destructive episodes in the building of a young Oceanic Island, La Palma, Canary Islands, and genesis of the Caldera de Taburiente, *J. Volc. Geotherm. Res.,* **60**(3-4), 243–262.

Anderson, D.L., 2001. Top-down tectonics?, *Science,* **293,** 2016–2018.

Backman, J., Duncan, R.A. & Party, S.S., 1988. Site 807, in *Proceedings to the ODP Sci. Res.,* Vol. **115,** pp. 233–399.

Bernard, A. & Munschy, M., 2000. Were the Mascarene and Laxmi Basins (western Indian Ocean) formed at the same spreading centre?: comptes Rendus de l'Academie des Sciences – Series IIA, *Earth planet. Sci.,* **330**(11), 777–783.

Bonneville, A., Barriot, J.P. & Bayer, R., 1988. Evidence from geoid data of a hotspot origin for the southern Mascarene Plateau and Mascarene Islands (Indian Ocean), *J. geophys. Res.,* **93,** 4199–4212.

Breton, T. *et al.*, 2013. Geochemical heterogeneities within the Crozet hotspot, *Earth planet. Sci. Lett.,* **376,** 126–136.

Bunce, E.T. & Chase, R.L., 1966. Preliminary results of the 1964 cruise of R.V. Chain to the Indian Ocean, *Phil. Trans. R. Soc. Lond. A,* **259**(1099), 218–226.

Burke, K.C. & Wilson, J.T., 1976. Hot spots on the Earth's surface, *J. geophys. Res.,* **93,** 7690–7708.

Burke, K.C., Steinberger, B., Torsvik, T. & Smethurst, M.A., 2008. Plume Generation Zones at the margins of Large Low Shear Velocity Provinces on the core–mantle boundary, *Earth planet. Sci. Lett.,* **265,** 49–60.

Cande, S.C. & Patriat, P., 2015. The anticorrelated velocities of Africa and India in the Late Cretaceous and early Cenozoic, *Geophys. J. Int.,* **200,** 227–243.

Cande, S.C. & Stegman, D.R., 2011. Indian and African plate motions driven by the push force of the Réunion plume head, *Nature,* **475,** 47–52.

Cande, S.C., Herron, E.M. & Hall, B.R., 1982. The Early Cenzoic tectonic history of the Southeast Pacific, *Earth planet. Sci. Lett.,* **57,** 63–74.

Cande, S.C., LaBrecque, J.L. & Haxby, W.F., 1988. Plate kinematics of the south Atlantic: Chron C34 to present, *J. geophys. Res.,* **93**(B11), 13 479–13 492.

Cande, S.C., Patriat, P. & Dyment, J., 2010. Motion between the Indian, Antarctic and African plates in the early Cenozoic, *Geophys. J. Int.,* **183,** 127–149.

Cantagrel, J.M., Cendrero, A., Fuster, J.M., Ibarrola, E. & Jamond, C., 1984. K-Ar chronology of the volcanic eruptions in the Canarian archipelago: island of La Gomera, *Bull. Volc.,* **47**(3), 597–609.

Chenet, A.L., Quidelleur, X., Fluteau, F., Courtillot, V. & Bajpai, S., 2007. 40K-40Ar dating of the Main Deccan large igneous province: further evidence of KTB age and short duration, *Earth planet. Sci. Lett.,* **263**(1-2), 1–15.

Coello, J. *et al.*, 1992. Evolution of the eastern volcanic ridge of the Canary Islands based on new K–Ar data, *J. Volc. Geotherm. Res.,* **53**(1–4), 251–274.

Collier, J.S., Sansom, V., Ishizuka, O., Taylor, R.N., Minshull, T.A. & Whitmarsh, R.B., 2008. Age of Seychelles-India break-up, *Earth planet. Sci. Lett.,* **272,** 264–277.

Conrad, C.P. & Behn, M.D., 2010. Constraints on lithosphere net rotation and asthenospheric viscosity from global mantle flow models and seismic anisotropy, *Geochem. Geophys. Geosyst.,* **11**(Q05W05), doi:10.1029/2009GC002970.

Copley, A., Avouac, J.-P. & Royer, J.Y., 2010. India-Asia collision and the Cenozoic slowdown of the Indian plate: implications for the forces driving plate motions, *J. geophys. Res.,* **115,** B03410, doi:10.1029/2009JB006634.

Courtillot, V., Davaille, A., Besse, J. & Stock, J., 2003. Three distinct types of hotspots in the Earth's mantle, *Earth planet. Sci. Lett.,* **205**(3-4), 295–308.

Cox, K.G., 1992. Karoo igneous activity, and the early stages of the break-up of Gondwanaland, in *Magmatism and the Causes of Continental Break-Up,* Vol. **68,** pp. 137–148, eds Storey, B.C., Alabaster, T. & Pankhurst, R.J., Geol. Soc. London.

Daly, M., Chorowicz, J. & Fairhead, J.D., 1989. Rift basin evolution in Africa: the influence of reactivated steep basement shear zones, *Geol. Soc. Lond. Spec. Publ.,* **44,** 309–334.

Deppe, J., Hauff, F., Hoernle, K., Werner, R., Garge-Schönberg, D., O'Connor, J.M. & Jokat, W., 2010. Evidence for a long-term geochemical zonation of the Tristan-Gough Hotspot, *Geophys. Res. Abstr.,* **12,** EGU2010–4314.

Doubrovine, V., Steinberger, B. & Torsvik, T.H., 2012. Absolute plate motions in a reference frame defined by moving hot spots in the Pacific, Atlantic, and Indian oceans, *J. geophys. Res.,* **117**(B9), B09101, doi:10.1029/2011JB009072.

Duncan, R.A., 1984. Age progressive volcanism in the New England seamounts and the opening of the central Atlantic Ocean, *J. geophys. Res.,* **89,** 9980–9990.

Duncan, R.A. & Clague, D.A., 1985. Pacific plate motion recorded by linear volcanic chains, in *The Ocean Basins and Margins,* Vol. **7A,** pp. 89–121, eds Nairn, A.E.M., Stehli, F.G. & Uyeda, S., Plenum.

Duncan, R.A. & Hargraves, R.B., 1990. 40Ar/39Ar Geochronology of basement rocks from the Mascarene Plateau, the Chagos Bank, and the Maldives Ridge, *Proc. ODP Sci. Res.,* **115,** 43–51.

Duncan, R.A. & Richards, M.A., 1991. Hotspots, mantle plumes, flood basalts, and true polar wander, *Rev. Geophys.,* **29**(1), 31–50.

Eagles, G. & Hoang, H.H., 2013. Cretaceous to present kinematics of the Indian, African and Seychelles plates, *Geophys. J. Int.,* **196**(1), 1–14.

Eagles, G. & Wibisono, A.D., 2013. Ridge push, mantle plumes and the speed of the Indian plate, *Geophys. J. Int.,* **194**(2), 670–677.

Emerick, C.M. & Duncan, R.A., 1982. Age progressive volcanism in the Comores Archipelago, western Indian Ocean and implications for Somali plate tectonics, *Earth planet. Sci. Lett.,* **60,** 415–428.

Fisher, R.L., Johnson, G.L. & Heezen, B.C., 1967. Mascarene Plateau, western Indian Ocean, *Geol. Soc. Am. Bull.,* **78,** 1247–1266.

Ganerød, M., 2011. Paleoposition of the Seychelles microcontinent in relation to the Deccan Traps and the plume generation zone in Late Cretaceous–Early Palaeogene time, in *The Formation and Evolution of Africa: A Synopsis of 3.8 Ga of Earth History,* Vol. **357,** pp. 229–252, eds Van Hinsbergen, D.J.J. *et al.*, Geol. Soc. Lond. Spec. Publ., The Geological Society of London.

Geldmacher, J., Hoernle, K., van den Bogaard, P., Zankl, G. & Garbe-Schonberg, D., 2001. Earlier history of the ≥70-Ma-old Canary hotspot based on the temporal and geochemical evolution of the Selvagen Archipelago and neighboring seamounts in the eastern North Atlantic, *J. Volc. Geotherm. Res.,* **111,** 55–87.

Geldmacher, J., Hoernle, K., Bogaard, P.v.d., Duggen, S. & Werner, R., 2005. New 40Ar/39Ar age and geochemical data from seamounts in the Canary and Madeira volcanic provinces: support for the mantle plume hypothesis, *Earth planet. Sci. Lett.,* **237**(1-2), 85.

Geldmacher, J., Hoernle, K., Klügel, A., Bogaard, P.v.d., Wombacher, F. & Berning, B., 2006. Origin and geochemical evolution of the Madeira-Tore Rise (eastern north Atlantic), *J. geophys. Res.,* **111**(B09206), doi:10.1029/2005JB003931.

Guillou, H., Carracedo, J.C., Torrado, F.P. & Badiola, E.R., 1996. K-Ar ages and magnetic stratigraphy of a hotspot-induced, fast grown oceanic island: El Hierro, Canary Islands, *J. Volc. Geotherm. Res.,* **73**(1-2), 141–155.

Guillou, H., Torrado, F.J.P., Hansen Machin, A.R., Carracedo, J.C. & Gimeno, D., 2004. The Plio–Quaternary volcanic evolution of Gran Canaria based on new K–Ar ages and magnetostratigraphy, *J. Volc. Geotherm. Res.,* **135**(3), 221–246.

Gurnis, M. *et al.*, 2012. Plate tectonic reconstructions with continuously closing plates, *Comput. Geosci.,* **38**(1), 35–42.

Hall, S. & Bird, D., 2007. Tristan da Cuhna hotspot tracks and the seafloor spreading history of the South Atlantic, *EOS, Trans. Am. geophys. Un.,* **88,** V31F-04.

Harada, Y. & Wessel, P., 2003. Motion of hotspots relative to the paleomagnetic axis, *EOS, Trans. Am. geophys. Un.,* **84**(46), Abstract V31F-04.

Heine, C. & Brune, S., 2014. Oblique rifting of the Equatorial Atlantic: why there is no Saharan Atlantic Ocean, *Geology,* **42**(3), 211–214.

Holm, P.M., Grandvuinet, T., Friis, J., Wilson, J.R., Barker, A.K. & Plesner, S., 2008. An 40Ar-39Ar study of the Cape Verde hot spot: temporal evolution in a semistationary plate environment, *J. geophys. Res.,* **113**(B0820), doi:10.1029/2007JB005339.

Iaffaldano, G., Hawkins, R., Bodin, T. & Sambridge, M., 2014. REDBACK: open-source software for efficient noise-reduction in plate kinematic reconstructions, *Geochem. Geophys. Geosyst.,* **15**(4), 1663–1670.

Koppers, A.A.P., Phipps Morgan, J., Morgan, J.W. & Staudigel, H., 2001. Testing the fixed hotspot hypothesis using 40Ar/39Ar age progressions along seamount trails, *Earth planet. Sci. Lett.,* **185,** 237–252.

Koppers, A.A.P. *et al.*, 2012. Limited latitudinal mantle plume motion for the Louisville hotspot, *Nat. Geosci,* **5,** doi:10.1038/ngeo1638.

Kumar, P., Yuan, X., Kumar, M.R., Kind, R., Li, X. & Chadha, R., 2007. The rapid drift of the Indian tectonic plate, *Nature,* **449**(7164), 894–897.

Livermore, R., Nankivell, A., Eagles, G. & Morris, P., 2005. Paleogene opening of Drake Passage, *Earth planet. Sci. Lett.,* **236**(1-2), 459–470.

McDougall, I., 1971. The geochronology and evolution of the young volcanic island of Réunion, Indian Ocean, *Geochim. Cosmochim. Acta,* **35,** 261–288.

McNutt, M.K., 1988. Thermal and mechanical properties of the Cape Verde Rise, *J. geophys. Res.,* **93**(B4), 2784–2794.

Meyerhoff, A.A. & Kamen-Kaye, M., 1981. Petroleum prospects of Saya de Malha and Nazareth Banks, Indian Ocean, *AAPG Bull.,* **65,** 1344–1347.

Milelli, L., Fourel, L. & Jaupart, C., 2012. A lithospheric instability origin for the Cameroon Volcanic Line, *Earth planet. Sci. Lett.,* **235-236,** 80–87.

Molnar, P. & Stock, J., 1987. Relative motions of hotspots in the Pacific, Atlantic and Indian Oceans since Late Cretaceous time, *Nature,* **327,** 587–591.

Morgan, J.W., 1981. Hotspot tracks and the opening of the Atlantic and Indian oceans, in *The Sea,* Vol. **7,** ed. Emiliani, C., Wiley.

Morra, G., Seton, M., Quevedo, L. & Müller, R.D., 2013. Organization of the tectonic plates in the last 200Myr, *Earth planet. Sci. Lett.,* **373,** 93–101.

Müller, R.D., Royer, J.-Y. & Lawver, L.A., 1993. Revised plate motions relative to the hotspots from combined Atlantic and Indian Ocean hotspot tracks, *Geology,* **21**(3), 275–278.

Müller, R.D., Royer, J.Y., Cande, S.C., Roest, W.R. & Maschenkov, S., 1999. New constraints on Carribean plate tectonic evolution, in *Caribbean Basins,* pp. 39–55, ed. Mann, P., Elsevier.

Müller, R.D., Sdrolias, M., Gaina, C. & Roest, W.R., 2008. Age, spreading rates, and spreading asymmetry of the world's ocean crust, *Geochem. Geophys. Geosyst.,* **9**(Q04006), doi:10.1029/2007GC001743.

Nürnberg, D. & Müller, R.D., 1991. The tectonic evolution of the South Atlantic from Late Jurassic to present, *Tectonophysics,* **191,** 27–53.

O'Connor, J.M. & Duncan, R.A., 1990. Evolution of the Walvis Ridge-Rio Grande Rise hot spot system: implications for African and South American plate motions of plumes, *J. geophys. Res.,* **95,** 17 475–417 502.

O'Connor, J.M. & LeRoex, A.P., 1992. South Atlantic hot spot-plume systems: 1. Distribution of volcanism in time and space, *Earth planet. Sci. Lett.,* **113**(3), 343–364.

O'Connor, J.M., Stoffers, P., van den Bogaard, P. & McWilliams, M., 1999. First seamount age evidence for significantly slower African plate motion since 19 to 30 Ma, *Earth planet. Sci. Lett.,* **171**(4), 575–589.

O'Connor, J.M., Jokat, W., le Roex, A.P., Class, C., Wijbrans, J.R., Keßling, S., Kuiper, K.F. & Nebel, O., 2012. Hotspot trails in the South Atlantic controlled by plume and plate tectonic processes, *Nat. Geosci.,* **5,** 735–738.

O'Connor, J.M. *et al.*, 2013. Constraints on past plate and mantle motion from new ages for the Hawaiian-Emperor Seamount Chain, *Geochem. Geophys. Geosyst*., **14**(10), 4564–4584.

O'Neill, C., Müller, D. & Steinberger, B., 2005. On the uncertainties in hot spot reconstructions and the significance of moving hot spot reference frames, *Geochem. Geophys. Geosyst.,* **6**(4), Q04003, doi:10.1029/2004GC000784.

Purdy, E.G. & Bertram, G.T., 1993. Carbonate concepts from the Maldives, Indian Ocean, *AAPG Stud. Geol.,* **34,** 1–56.

Raymond, C.A., Stock, J.M. & Cande, S.E., 2000. Fast Paleogene motion of the Pacific hotspots from revised global plate curcuit constraints, in *The History and dynamics of Global Plate Motions,* Vol. **121,** pp. 359–375, eds Richards, M.A., Gordon, R.G. & van der Hilst, R.D., AGU.

Reusch, A.M., Nyblade, A.A., Tibi, R., Wiens, D.A., Shore, P.J., Bekoa, A., Tabod, C.T. & Nnange, J.M., 2011. Mantle transition zone thickness beneath Cameroon: evidence for an upper mantle origin for the Cameroon Volcanic Line, *Geophys. J. Int.,* **187,** 1146–1150.

Rohde, J.K., van den Bogaard, P., Hoernle, K., Hauff, F. & Werner, R., 2013. Evidence for an age progression along the Tristan-Gough volcanic track from new 40Ar/39Ar ages on phenocryst phases, *Tectonophysics,* **604,** 60–71.

Royer, J.Y., Gordon, R.G. & Horner-Johnson, B.C., 2006. Motion of Nubia relative to Antarctica since 11 Ma: implications for Nubia-Somalia, Pacific-North America, and India-Eurasia motion, *Geology,* **34,** 501–504.

Sager, W.W. & Tominaga, M., 2008. Paleomagnetism of basaltic rocks cored from the Walvis Ridge, South Atlantic and implications for Hotspot Paleolatitude, *EOS, Trans. Am. geophys. Un.,* **89,** Abstract GP14A-05.

Schlich, R., 1982. The Indian Ocean: aseismic ridges, spreading centres and basins, The Ocean Basins and Margins, in *The Indian Ocean,* Vol. **6,** pp. 51–147, Plenum.

Seton, M. *et al.*, 2012. Global continental and ocean basin reconstructions since 200 Ma, *Earth Sci. Rev.,* **113,** 212–270.

Sharp, W.D. & Clague, D.A., 2006. 50-Ma initiation of Hawaii-Emperor bend records major change in Pacific plate motion, *Science,* **313,** 1281–1284.

Skolotnev, S.G., Bel'tenev, V.E., Lepekhina, E.N. & Ipat'eva, I.S., 2010. Younger and Older Zircons from Rocks of the Oceanic Lithosphere in the Central Atlantic and Their Geotectonic Implications, *Geotectonics,* **44**(6), 462–492.

Small, C., 1995. Observations of ridge-hotspot interactions in the southern ocean, *J. geophys. Res,* **100**(B9), 17 931–17 946.

Steinberger, B., Sutherland, R. & O'Connell, R.J., 2004. Prediction of Emperor-Hawaii seamount locations from a revised model of global plate motion and mantle flow, *Nature,* **430,** 167–173.

Tarduno, J.A., Bunge, H.-P., Sleep, N.H. & Hansen, U., 2009. The bent Hawaiian-Emperor hotspot track: inheriting the mantle wind, *Science,* **324,** 50–53.

Tarduno, J.A. *et al.*, 2003. The emperor seamounts: southward motion of the Hawaiian Hotspot Plume in Earth's mantle, *Science,* **301**(5636), 1064–1069.

Thirlwall, M.F., Singer, B.S. & Marriner, G.F., 2000. 39Ar–40Ar ages and geochemistry of the basaltic shield stage of Tenerife, Canary Islands, Spain, *J. Volc. Geotherm. Res.,* **103,** 247–297.

Tiwari, V.M., Grevemeyer, I., Singh, B. & Phipps Morgan, J., 2007. Variation of effective elastic thickness and melt production along the Deccan–Reunion hotspot track, *Earth planet. Sci. Lett.,* **264,** 9–21.

Torsvik, T., Tucker, R.D., Ashwal, L.D., Eide, E.A., Rakotosolofo, N.A. & de Wit, M.J., 1998. Late Cretaceous magmatism in Madagascar: palaeomagnetic evidence for a stationary Marion hotspot, *Earth planet. Sci. Lett.,* **164,** 221–232.

Torsvik, T., Müller, R.D., Van der Voo, R., Steinberger, B. & Gaina, C., 2008. Global plate motion frames: toward a unified model, *Rev. Geophys.,* **46**(RG3004), doi:10.1029/2007RG000227.

Torsvik, T.H., Steinberger, B., Gurnis, M. & Gaina, C., 2010. Plate tectonics and net lithosphere rotation over the past 150 My, *Earth planet. Sci. Lett.,* **291**(1-4), 106–112.

Torsvik, T.H. *et al.*, 2013. A Precambrian microcontinent in the Indian Ocean, *Nat. Geosci.,* **6,** 223–227.

Torsvik, T.H. *et al.*, 2014. Deep mantle structure as a reference frame for movements in and on the Earth, *Proc. Nat. Acad. Sci.,* **11**(24), 8735–8740.

Tucholke, B.E. & Smoot, N.C., 1990. Evidence for age and evolution of Corner seamounts and Great Meteor seamount chain from multibeam bathymetry, *J. geophys. Res.,* **95**(B11), 17 555–17 569.

van Hinsbergen, D.J.J., Steinberger, B., Doubrovine, P.V. & Gassmöller, R., 2011. Acceleration and deceleration of India-Asia convergence since the Cretaceous: roles of mantle plumes and continental collision, *J. geophys. Res.,* **116**(B6), B06101, doi:10.1029/2010JB008051.

Vandamme, D. & Courtillot, V., 1990. Latitudinal evolution of the Réunion hotpsot deduced from paleomagnetic results of Leg 115, *Geophys. Res. Lett.,* **17**(8), 1105–1108.

Wessel, P. & Kroenke, L.W., 2008. Pacific absolute plate motions since 145 Ma: an assessment of the fixed hotspot hypothesis, *J. geophys. Res.,* **113**(B06101), doi:10.1029/2007JB005499.

Wessel, P. & Kroenke, L.W., 2009. Observations of geometry and ages constrain relative motion of Hawaii and Louisville plumes, *Earth planet. Sci. Lett.,* **284**(3/4), 467–472.

Wessel, P., Harada, Y. & Kroenke, L.W., 2006. Towards a self-consistent, high-resolution absolute plate motion model for the Pacific, *Geochem. Geophys. Geosyst.,* **7**(Q03L12), doi:10.1029/2005GC001000.

Whittaker, J.M., Muller, R.D., Leitchenkov, G., Stagg, H., Sdrolias, M., Gaina, C. & Goncharov, A., 2007. Major Australian-Antarctic Plate reorganization at Hawaiian-Emperor bend time, *Science,* **318**(5847), 83–86.

Whittaker, J.M., Williams, S.E. & Müller, R.D., 2013. Revised tectonic evolution of the Eastern Indian Ocean, *Geochem., Geophys., Geosyst.,* **14**(6), 1891–1909.

SUPPORTING INFORMATION

Additional Supporting Information may be found in the online version of this paper:

Figure S1a. Mascarene fit APM at 5 Ma.
Figure S1b. Chagos-Laccadive fit APM at 5 Ma.
Figure S2a. Mascarene fit APM at 10 Ma.
Figure S2b. Chagos-Laccadive fit APM at 10 Ma.
Figure S3a. Mascarene fit APM at 15 Ma.
Figure S3b. Chagos-Laccadive fit APM at 15 Ma.
Figure S4a. Mascarene fit APM at 20 Ma.
Figure S4b. Chagos-Laccadive fit APM at 20 Ma.
Figure S5a. Mascarene fit APM at 25 Ma.
Figure S5b. Chagos-Laccadive fit APM at 25 Ma.
Figure S6a. Mascarene fit APM at 30 Ma.
Figure S6b. Chagos-Laccadive fit APM at 30 Ma.
Figure S7a. Mascarene fit APM at 35 Ma.
Figure S7b. Chagos-Laccadive fit APM at 35 Ma.
Figure S8a. Mascarene fit APM at 40 Ma.
Figure S8b. Chagos-Laccadive fit APM at 40 Ma.
Figure S9a. Mascarene fit APM at 45 Ma.
Figure S9b. Chagos-Laccadive fit APM at 45 Ma.
Figure S10a. Mascarene fit APM at 50 Ma.
Figure S10b. Chagos-Laccadive fit APM at 50 Ma.
Figure S11a. Mascarene fit APM at 55 Ma.
Figure S11b. Chagos-Laccadive fit APM at 55 Ma.
Figure S12a. Mascarene fit APM at 60 Ma.
Figure S12b. Chagos-Laccadive fit APM at 60 Ma.
Figure S13a. Mascarene fit APM at 65 Ma.
Figure S13b. Chagos-Laccadive fit APM at 65 Ma.
Figure S14a. Mascarene fit APM at 70 Ma.
Figure S14b. Chagos-Laccadive fit APM at 70 Ma.
Figure S15a. Mascarene fit APM at 75 Ma.
Figure S15b. Chagos-Laccadive fit APM at 75 Ma.
Figure S16a. Mascarene fit APM at 80 Ma.
Figure S16b. Chagos-Laccadive fit APM at 80 Ma.

Table S1. Absolute plate motion model A of Africa (Mascarene fit), with uncertainties. The angle is given in degrees, Ages are in Ma, and *a–f* is given in rad^2. For the uncertainties $\hat{k}$ is set to 1 and g to 10^{-5}. Covariance estimates for the i'th rotation are given by

$$c_i = cov(\mathbf{r}_i) = \frac{1}{k}\begin{bmatrix} a_i & b_i & d_i \\ b_i & c_i & e_i \\ d_i & e_i & f_i \end{bmatrix} g.$$

Table S2. Absolute plate motion model B of Africa (Chagos-Laccadive fit), with uncertainties (see Table S1 for details).
Table S3. Unsmoothed absolute plate motion model A of Africa (Mascarene fit), with uncertainties (see Table S1 for details).
Table S4. Unsmoothed absolute plate motion model B of Africa (Chagos-Laccadive fit), with uncertainties (see Table S1 for details) (http://gji.oxfordjournals.org/lookup/suppl/doi:10.1093/gji/ggv104/-/DC1).

Please note: Oxford University Press is not responsible for the content or functionality of any supporting materials supplied by the authors. Any queries (other than missing material) should be directed to the corresponding author for the paper.